Experimental And Theoretical Investigation On Hot Mix Asphalts Outflow Times: Boundary Conditions Influence

---

Praticò Filippo G.
Associate Professor, DIMET Department Of Computer Science Mathematics Electronics And Transportation,
Reggio Calabria Mediterranean University - fpratico@ing.unirc.it

Moro A.
Ph.D. Student, DIMET Department Of Computer Science Mathematics Electronics And Transportation,
Reggio Calabria Mediterranean University - amoro@ing.unirc.it

Synopsis

The goal of this paper is confined to the permeability and drainability of Hot Mix Asphalts (HMA), as key-characteristics for pavement reliability. As is well known, these parameters may be considered very important in assessing both surface performance (wet friction, splash and spray, raveling, stripping, etc.) and mechanistic properties (resistance and moduli dependence on water action).

Authors formalize a physical-based model to analyze the phenomena of water flows for different typologies of friction courses (Dense Friction Courses, Open Graded Friction Courses, Porous Asphalts, etc.).

On the basis of the formalized models, a specific experimental plan was designed and performed, in order to analyze the relationships among the main parameters of the model.

Boundary conditions influence on outputs was deeply investigated, by considering different methods in obtaining outflow times.

The focal applications of the study, both theoretical and experimental, are the following two: a) assessment of a relation between composition and drainability; b) estimation of the relative influence of some boundary conditions.

Experimental And Theoretical Investigation On Hot Mix Asphalts Outflow Times: Boundary Conditions Influence

As is well known, permeability and drainability are very important properties that influence both surface performance (wet friction, splash and spray, raveling, stripping, etc.) and mechanistic characteristics (resistance and moduli) of HMA (Hot Mix Asphalt).

These parameters are a function of HMA components (such as aggregate gradation, asphalt content, air voids, etc.) and compaction procedures.

Because of the presence of many field and laboratory methods and devices used for calculating permeability and drainability values, in this study particular attention is turned towards boundary conditions influence on results.

INFLUENCE OF HMA VOLUMETRICS ON PERMEABILITY AND DRAINABILITY

It is known that, in the various HMAs, air voids range from 2% to more than 25% (see Table 1). These large variations origin from and influence different performance requirements.

Tab 1

PAVEMENT TYPE	AIR VOIDS (%)
Fine-Graded + Coarse-Graded Friction Courses (DGFC)	3 ÷ 7
European Binder Courses (EBC)	4 ÷ 7
European Base Courses (EBAC)	4 ÷ 8
Stone Mastic Asphalts (SMA)	2 ÷ 6
First Generation Open-Graded Friction Courses (OGFC)	10 ÷ 15
New Generation Open-Graded Friction Courses (OGFC)	> 18
Asphalt-Rubber Friction Courses (ARFC)	> 18
Porous European Mixes (PEM)	18 ÷ 25

Several researches in different conditions has been conducted to evaluate the factors that influence HMA permeability and drainability.

In these studies different methods and devices (both in-lab and in-field) to estimate outflow times and permeability values were utilized.

Also, different fluids (air, water, saline solutions, etc.) have been used and mixes with different properties (asphalt content, aggregate gradation, percent air voids, thickness) have been compacted (using different laboratory and field procedures) and tested.

In Table 2 (see the Appendices) a review of the international literature on HMA permeability is summarized.

On the basis of the considered main categories the following observations may be drown:

- Many Pavement types are considered (Fine -, Coarse-graded, Stone Mastic Asphalt-SMA, Open Graded Friction Courses-OGFC, Superpave mixes, etc.);
- The considered Air voids range is very large (< 8%, 8% ≈ 12%, 13% ≈ 20%, 20% ≈ 23%);
- Thickness ranges from 2 to 10 cm;
- The Nominal Maximum Aggregate Size range from 9,5 mm to 25 mm;
- Different Compaction Procedures (in-place, in-lab, by rollers, giratory compactors, etc) are considered;
- Many Devices and Indicators are used (vertical, horizontal permeability, drainability, others);
- Different fluids can be used (H_2O, air, NaCl, $NaCl_2$, $MgCl_2$, etc.);
- The range of the measured indicator is very large (as air void increases from 4 to 22% permeabilities range from 10^{-5} to 1 cm/s, see Figure 1).

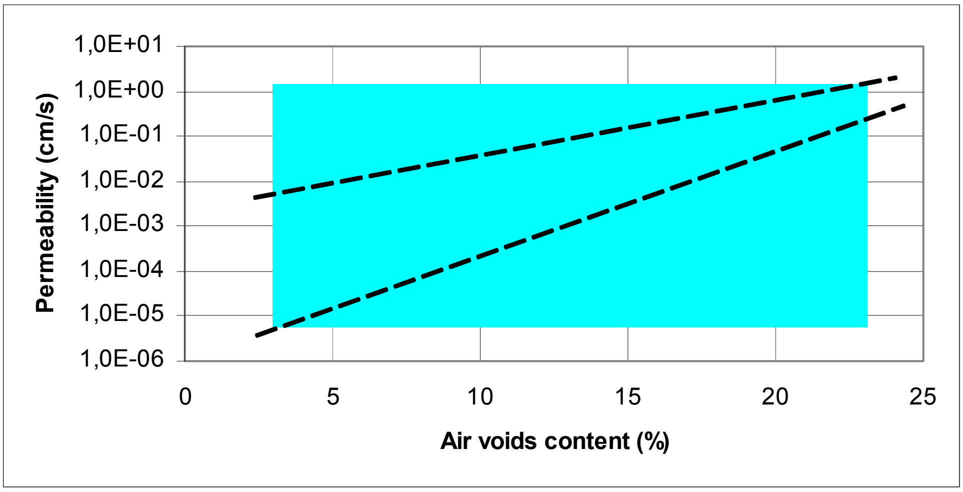

Figure 1: Influence of air voids on permeability

AIR VOIDS/OUTFLOW TIMES RELATIONSHIPS WITH MECHANICAL PROPERTIES

It is well know that air voids and outflow times may be considered strictly referenced to HMA mechanical properties. Table 3 (see the Appendices) summarizes the analysis of the international literature on this topic. By doubling the air voids content from 5% to 10% (see Figure 2) the fatigue life (F) has a loss of about 70%, Moduli (M) decay of about 30%, Rutting rate (R) is doubled, the bitumen viscosity in 10-years old surface courses (V) increases with a factor 1,5.
These “enormous” changes can correspond to a slight change in asphalt density (D) (about 5%).

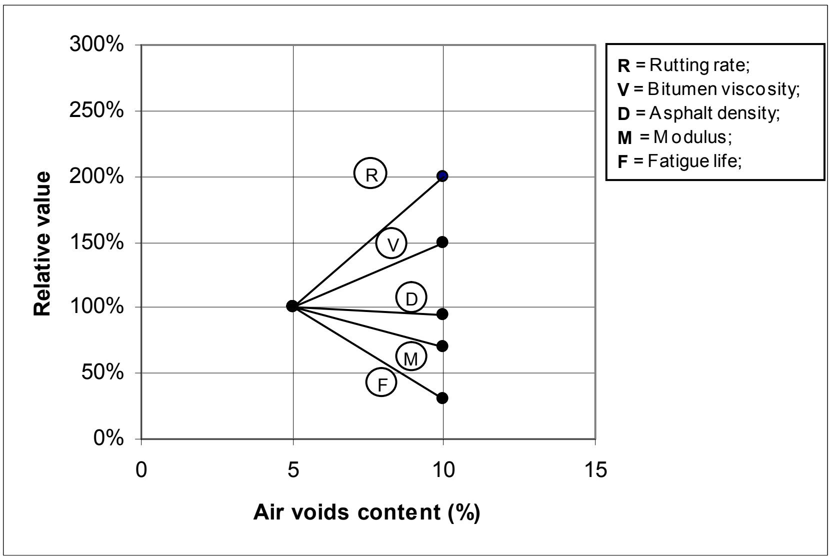

Figure 2: Change in service properties at varying levels of in-field air voids - a summary

PROBLEM MODELING

On the basis of the analysis of the international literature, most of the existing models for water flow in HMA may be grouped as it follows (PRATICO’ et al., 2005):

- models based on the analysis of casual motions;
- models based on one-dimensional and laminar flows under the validity of Darcy’s law;
- models based on continuity equation (or Richards equation (APUL et al., 2002)), Darcy’s law (sometimes modified) and vertical water saturation front;
- models based on Kozeny-Carman equation;
- models based on continuity equation, Darcy’s law, degree of saturation and drainable porosity (APUL et al., 2002);
- models that couple mass and heat balances with mechanical deformation (considering air and water flow in a porous media, vapor diffusion, liquid-vapor phase changes, (APUL et al., 2002));
- integrated models (integration of other existing models, for example, precipitation model, infiltration and drainage model, climatic-materials-structural model) (APUL et al., 2002);

- other models, such as for example, mixture theory formulation (after MURALI et al., 2001) or models based on the relationship between permeability and air void size distribution (after CASTELBLANCO et al., 2005).

The theoretical model here developed to investigate the flow of water through/over HMA pavements is still based on the continuity equation. It presents an equation for calculating the outflow times (see Figure 3). The parameter *a* (main parameter of the model) is expressed as a function of percent air voids in HMA and pavement thickness. The total flow rate Q_T is a function of four main parameters.

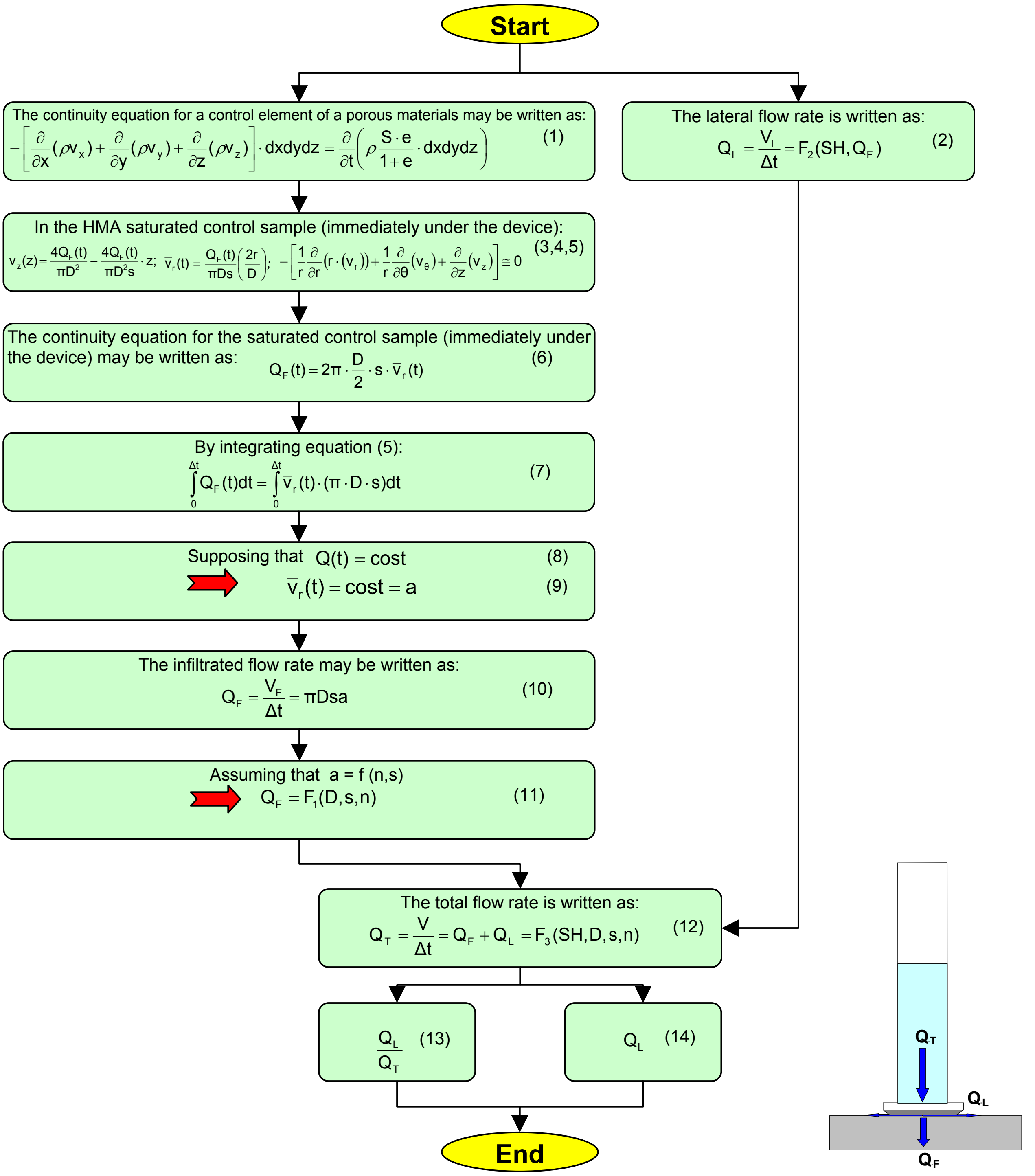

The continuity equation for a control element of a porous materials may be written as:

$$-\left[\frac{\partial}{\partial x}(\rho v_x)+\frac{\partial}{\partial y}(\rho v_y)+\frac{\partial}{\partial z}(\rho v_z)\right]\cdot dxdydz=\frac{\partial}{\partial t}\left(\rho\frac{S\cdot e}{1+e}\cdot dxdydz\right) \quad (1)$$

The lateral flow rate is written as:

$$Q_L=\frac{V_L}{\Delta t}=F_2(SH,Q_F) \quad (2)$$

In the HMA saturated control sample (immediately under the device):

$$v_z(z)=\frac{4Q_F(t)}{\pi D^2}-\frac{4Q_F(t)}{\pi D^2 s}\cdot z;\ \ \bar{v}_r(t)=\frac{Q_F(t)}{\pi Ds}\left(\frac{2r}{D}\right);\ \ -\left[\frac{1}{r}\frac{\partial}{\partial r}(r\cdot(v_r))+\frac{1}{r}\frac{\partial}{\partial \theta}(v_\theta)+\frac{\partial}{\partial z}(v_z)\right]\cong 0 \quad (3,4,5)$$

The continuity equation for the saturated control sample (immediately under the device) may be written as:

$$Q_F(t)=2\pi\cdot\frac{D}{2}\cdot s\cdot\bar{v}_r(t) \quad (6)$$

By integrating equation (5):

$$\int_0^{\Delta t}Q_F(t)dt=\int_0^{\Delta t}\bar{v}_r(t)\cdot(\pi\cdot D\cdot s)dt \quad (7)$$

Supposing that $Q(t)=cost$ (8)

$\Rightarrow \bar{v}_r(t)=cost=a$ (9)

The infiltrated flow rate may be written as:

$$Q_F=\frac{V_F}{\Delta t}=\pi Dsa \quad (10)$$

Assuming that a = f (n,s)

$\Rightarrow Q_F=F_1(D,s,n)$ (11)

The total flow rate is written as:

$$Q_T=\frac{V}{\Delta t}=Q_F+Q_L=F_3(SH,D,s,n) \quad (12)$$

$\frac{Q_L}{Q_T}$ (13)

Q_L (14)

SYMBOLS
a = parameter of the model; D = Permeameter opening diameter; Δt = outflow time; e = void ratio; n = percent air voids; $Q_F(t)$ = filtered flow rate at the time t; $Q_L(t)$ = lateral flow rate at the time t; $Q_T(t)$ = total flow rate at the time t ; r = radial direction; ρ = water density; s = HMA pavement thickness; S = degree of saturation; SH = Sand Height; V_F = filtered water volume; V_L = sideways flowed water volume; V = total water volume between timing marks; v_r = radial velocity; v_θ = angular velocity; v_x = velocity in the direction x; v_y = velocity in the direction y; v_z = velocity in the direction z (vertical);

Figure 3: Scheme of the formalized model

EXPERIMENTAL INVESTIGATION

Experimental plan

This section deals with the specific experimental plan designed in order to investigate boundary conditions influence on the relationships among the main parameters of the model, outflow times and HMA properties. Figure 4 resumes the experimental plan for the i-th mix and the k-th location (symbols are explained in Table 4).

Two HMA types were considered: Dense Graded Friction Courses (DGFC, locations k from 1 to 7) and Porous European Mixes (PEM, locations k from 8 to 22).

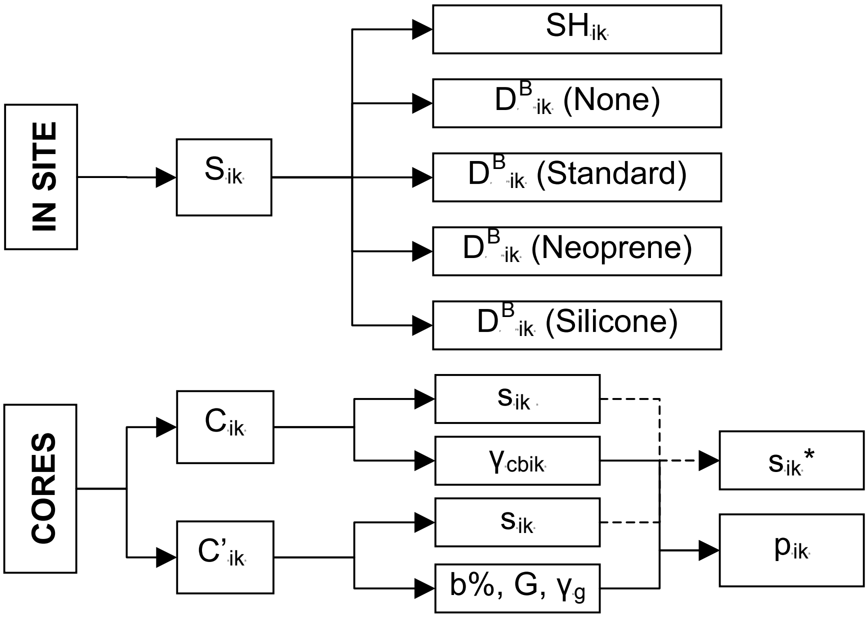

Figure 4: Experimental plan for the i-th mix and the k-th location (see table 3)

Table 4 summarizes the methods and devices used for measuring outflow times, drainability values and HMA properties. Figure 5 shows the mean gradation of the used bituminous mixes. Figures 6 to 10 refer to the main phases and devices of in-place experiments.

Tab 4: Standards , devices and symbols in Figure 4

INDICATOR	STANDARD	DEVICE
D^B_{ik}(Standard) = drainability measured in test location k for mix i (with cellular rubber base)	CME 54.17	Belgian permeameter
D^B_{ik}(none) = drainability measured in test location k for mix i (without base)		Belgian permeameter
D^B_{ik}(Neoprene) = drainability measured in test location k for mix i (with neoprene base)		Belgian permeameter
D^B_{ik}(Silicone) = drainability measured in test location k for mix i (with silicone and without base)		Belgian permeameter
SH_{ik} = Sand Height measured in test location k for mix i	C.N.R. BU N.94 – 1983	
b% = asphalt content	C.N.R. BU N.38 - 1973	
G = aggregate gradation	C.N.R. BU N.23	
γ_g = aggregate bulk density	C.N.R. BU N.63-1978	
γ_{cbik} = mixture bulk density of core C_{ik}	C.N.R BU N.40-1973	
S_{ik} = k-th in-field test location for the i-th mix (with i related to Dense Graded Friction Courses or Porous European Mixes);		
s_{ik} = thickness of core C_{ik}		
s^*_{ik} = average thickness of core C_{ik}		
C_{ik} = cores extracted in test location k;		
p_{ik} = air voids in site;	C.N.R. BU N.39 -1973	

Table 5 lists the main physical and chemical properties of the three different bases used under the drainometer in the experiments (LAUREN, 2005).

Tab 5: Material characteristics of the different bases

Condition	Standard		
Material	**Cellular rubber SBR**	**Neoprene**	**Silicone**
Physical Properties			
Density (g/cm^3)	0,94	1,23	0,95 to 1,20
Tensile Strength	F-G	VG	F-G
Elongation	G	G	VG-E
Compression Set	G	F-G	G-E
Heat Resistance	F-G	F-G	E
Resilience or Rebound	F-G	VG	G
Impact Resistance	E	G	P-G
Abrasion Resistance	G-E	G-E	P-F
Tear Resistance	F	F-G	P-F
Cut Growth	G	G	P-F
Flame Resistance	P	G	F-G
Impermeability, Gas	F	F-G	F-G
Weathering Resistance	F	VG	F
Low Temperature Limit	-17,8° to -45,6°C	-23,3° to -45,6°C	-53,9 to -101,1 °C
High Temperature Limit	70° to 107,2°C	107,2°C	204,4 to 287,8 °C
Chemical Resistance Properties			
Acid	F-G	G	F
Alcohols	G	VG	G
Aliphatic Hydrocarbon Solvents	P	G	P-F
Alkali	F	E	P
Animal & Vegetable	F	G	G
Aromatic Hydrocarbon Solvents	P	P-F	P-F
Oil & Gasoline	P	F-G	P-F
Oxygenated Solvents	G	P-F	F
Water	G-E	G	G-E
E=Excellent; VG=Very Good; G=Good; F=Fair; P=Poor			

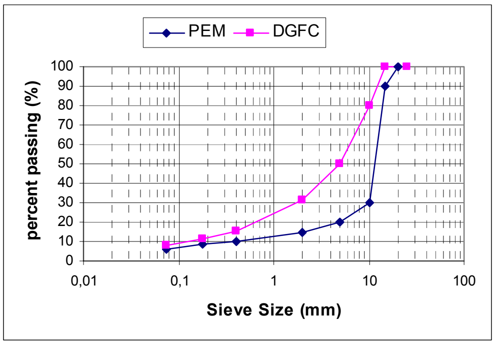

Figure 5: DGFC and PEM gradations

Figure 6: Belgian Permeameter (B, without base)

Figure 7: Neoprene base for device B

Figure 8: Cellular rubber base (Standard) for device B

Figure 9: Sand Patch method

Figure 10: Device B, Silicone

Results And Discussion

The obtained results are summarized in Table 6. It shows the influence of boundary conditions (in terms of None, Standard, Neoprene and Silicone bases) on outflow times (and relative components Q_T, Q^*_L, Q^*_F herein explained) at the different k locations (1 to 7 for DGFC and 8 to 22 for PEM), each one with a proper SH (Sand Height, mm). Before examining the results it is necessary to remark what follows:

- average flow rates are here considered; a mark 5 cm far from the uppermark of Belgian drainometer was identified;
- $(Q)_{Tj}$ stands for total flow rate (cm^3/s). It was measured for the j-th boundary condition (None, Standard, Neoprene, Silicone);
- $Q_{silicone}$ is the total flow rate (cm^3/s) when base is sealed by silicone;
- if one hypothesizes that $Q_{silicone} = Q_F^*$ (where Q^*_F stands for approximated filtered flow rate), then it is $Q_L^* = Q_T - Q_{silicone}$ and $\frac{Q_L^*}{Q_T} = 1 - \frac{Q_{silicone}}{Q_T}$ where Q^*_L stands for the approximation of the horizontal flow rate and L stands for lateral;
- on the contrary $(Q_T)_j$ values (measured) are without apex star because they are not affected by the above cited hypothesis;
- more in general, for the j-th boundary condition, it comes $\left(Q_L^*\right)_j = (Q)_{Tj} - Q_F^*$;
- it is well known that HMA surface texture influences outflow times: by changing the boundary conditions from "Silicone" to "None" the total flow $(Q_T)_j$ (that is to say lateral + filtered, for the j-th boundary condition) may have appreciable variations; therefore a specific study is herein performed.

Figure 11 to 34 resume the obtained results. By observing figures 11 to 13, referred to boundary conditions influence on the Q_T, it appears quite evident that the manner in which the base is fitted can greatly modify the results. In particular, for the DGFCs by passing from the j-th to the (j+1)-th boundary condition Q_T results about ten times greater. Total flow rates for "None" conditions ranges all from 100 cm^3/s to 700 cm^3/s (horizontal drainability influence).

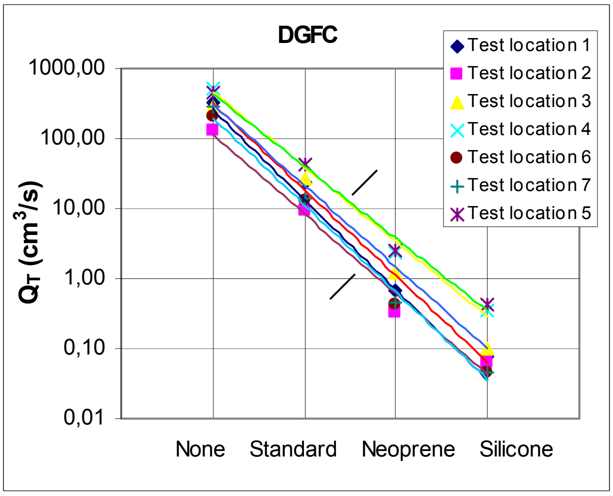

Figure 11: Q_{TJ} (DGFC)

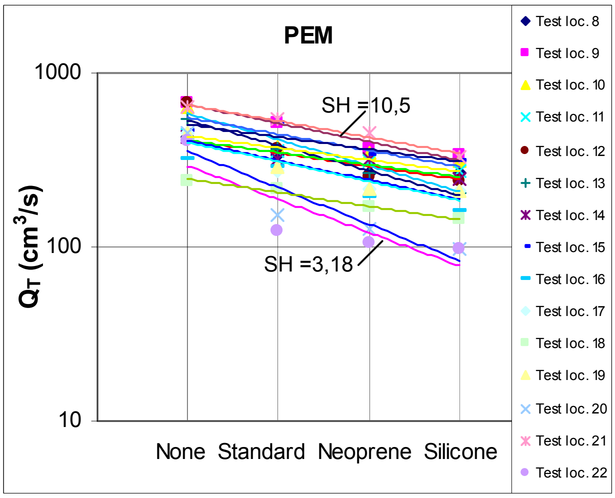

Figure 12: Q_{TJ} (PEM)

Figure 13: Q_{TJ} (DGFC and PEM)

Tab 6: Results

	Dense Graded Friction Course (DGFC)							Porous European Mixes (PEM)														
Test location	1	2	3	4	5	6	7	8	9	10	11	12	13	14	15	16	17	18	19	20	21	22
$(Q_T)_{None}$	321,29	131,93	284,42	502,88	468,90	209,03	294,06	433,74	680,37	630,89	444,86	667,29	550,78	423,16	462,65	318,34	450,63	240,96	450,63	456,56	630,89	403,48
$(Q_T)_{Standard}$	22,92	9,55	26,98	41,81	43,76	12,85	13,63	333,64	510,28	373,11	357,72	365,25	369,14	321,29	510,28	289,16	273,22	212,88	289,16	153,53	542,17	123,05
$(Q_T)_{Neoprene}$	0,69	0,32	1,21	2,41	2,51	0,43	0,45	266,91	369,14	343,55	315,44	255,14	264,88	318,34	333,64	196,04	212,88	169,26	216,87	128,51	456,56	105,79
$Q_{Silicone}$	0,08	0,06	0,10	0,35	0,43	0,05	0,05	262,87	333,64	315,44	275,39	239,30	204,11	247,85	309,81	159,90	207,78	143,38	207,78	97,47	327,35	98,30
SH (mm)	1,08	0,71	1,02	1,61	1,44	0,87	0,91	6,40	10,52	5,74	6,14	4,68	5,51	5,89	5,66	5,89	4,97	4,41	4,79	2,89	7,20	3,18
$(Q^*_L)_{Standard}$	22,84	9,48	26,88	41,46	43,32	12,81	13,59	70,77	176,63	57,66	82,33	125,95	165,03	73,44	200,47	129,25	65,44	69,49	81,38	56,07	214,82	24,75
$(Q^*_L)_{None}$	321,21	131,87	284,31	502,54	468,47	208,98	294,01	170,87	346,73	315,44	169,47	427,98	346,66	175,31	152,84	158,44	242,86	97,58	242,86	359,10	303,54	305,18
$(Q^*_L)_{Neoprene}$	0,61	0,26	1,11	2,06	2,07	0,38	0,41	4,04	35,49	28,11	40,06	15,84	60,77	70,49	23,83	36,14	5,10	25,88	9,09	31,05	129,22	7,49
$(Q^*_L)_{silicone}$	0	0	0	0	0	0	0	0	0	0	0	0	0	0	0	0	0	0	0	0	0	0
$(Q_T)_{None}/Q_{silicone}$	4062,8	2158,3	2752,4	1450,2	1080,4	4637,6	6395,8	1,65	2,04	2,00	1,62	2,79	2,70	1,71	1,49	1,99	2,17	1,68	2,17	4,68	1,93	4,10
$(Q^*_L/Q_T)_{Standard}$	0,997	0,994	0,996	0,992	0,990	0,996	0,997	0,212	0,346	0,155	0,230	0,345	0,447	0,229	0,393	0,447	0,240	0,326	0,281	0,365	0,396	0,201
$(Q^*_L/Q_T)_{None}$	0,9998	0,9995	0,9996	0,9993	0,9991	0,9998	0,9998	0,3939	0,5096	0,5000	0,3810	0,6414	0,6294	0,4143	0,3304	0,4977	0,5389	0,4050	0,5389	0,7865	0,4811	0,7564
$(Q^*_L/Q_T)_{Neoprene}$	0,886	0,810	0,915	0,856	0,827	0,894	0,899	0,015	0,096	0,082	0,127	0,062	0,229	0,221	0,071	0,184	0,024	0,153	0,042	0,242	0,283	0,071
$(Q^*_L/Q_T)_{silicone}$	0	0	0	0	0	0	0	0	0	0	0	0	0	0	0	0	0	0	0	0	0	0
Δt_B (s)	78,5	189,2	65,7	43,5	41,4	140,9	134	5,1	3,7	4,6	4,8	4,2	4,6	5,1	3,9	6,6	5,7	7,2	5,8	10,7	3,0	13,5

Note: Flow rates are in cm^3/s

Figures 14 to 16 compare the two extreme boundary conditions (none – without base, and silicone – perfectly sealed). The total flow rate ratio ranges from 1000 to about six time this value for DGFC.
On the contrary, for the PEMs, this ratio ranges from 1,5 to 5. R-square coefficients rise from 0,5 to 0,9 when both the HMA types are considered.

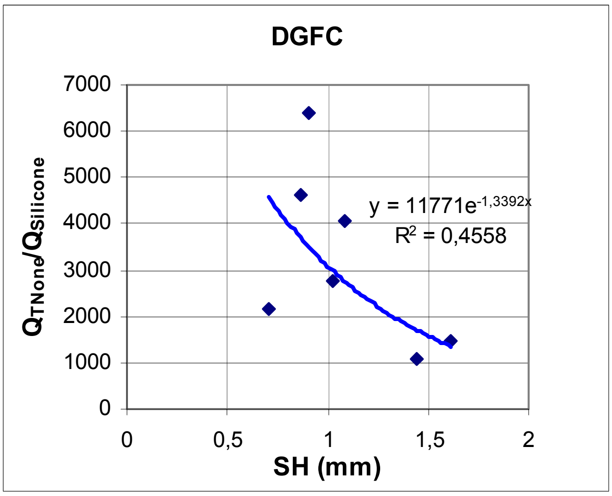

Figure 14: $Q_{TNone}/Q_{TSilicone}$ (DGFC)

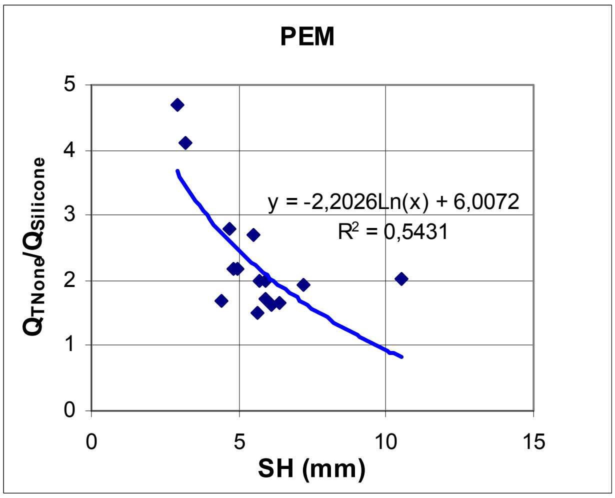

Figure 15: $Q_{TNone}/Q_{TSilicone}$ (PEM)

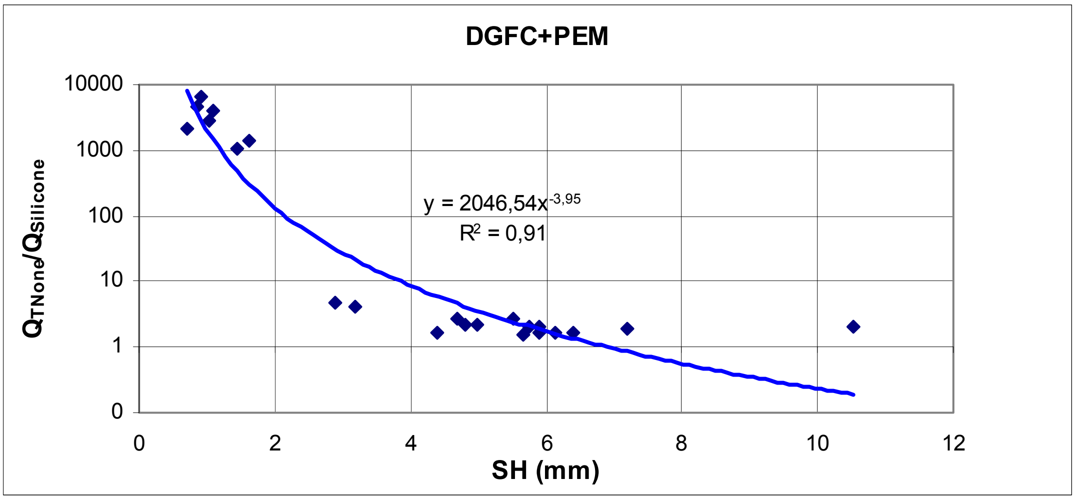

Figure 16: $Q_{TNone}/Q_{TSilicone}$ (DGFC and PEM)

Figures 17 to 19 deal with SH influence on the total flow rate, for four boundary conditions and two mix types (DGFC and PEM). Points appear quite well fitted by the different interpolating curves; both for DFGC, PEM and DFGC+PEM plots the correlations are positive and the R-square coefficients are quite high (from 0,72 to 0,97).

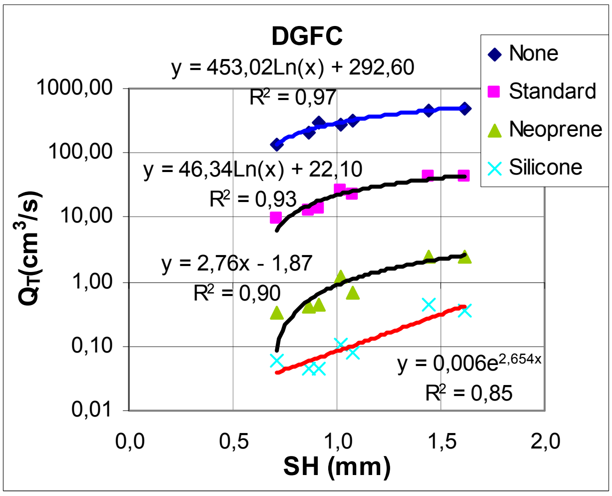

Figure 17: Q_T versus SH (DGFC)

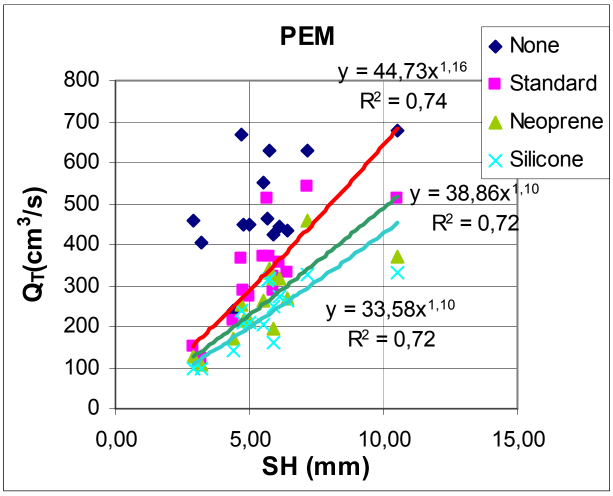

Figure 18: Q_T versus SH (PEM)

"None" curves are higher than standard ones, standard curves are higher than Neoprene ones, and silicone values are the lowest.

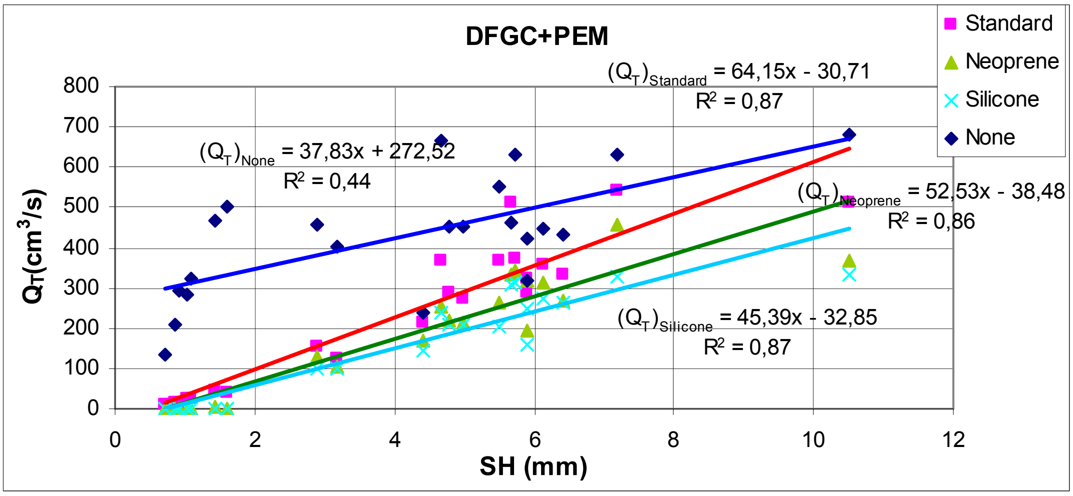

Figure 19: Q_T versus SH (DGFC+ PEM)

The scope of the figures 20 to 22 is to evaluate the influence of macro-texture on the horizontal (lateral) flow rates, when neoprene bases are used (softer than the standard). As one can observe, correlations are positive but R-square coefficients are not always high; for very high Sand Heights, points are quite scattered from the best-fitting curves (PEM).

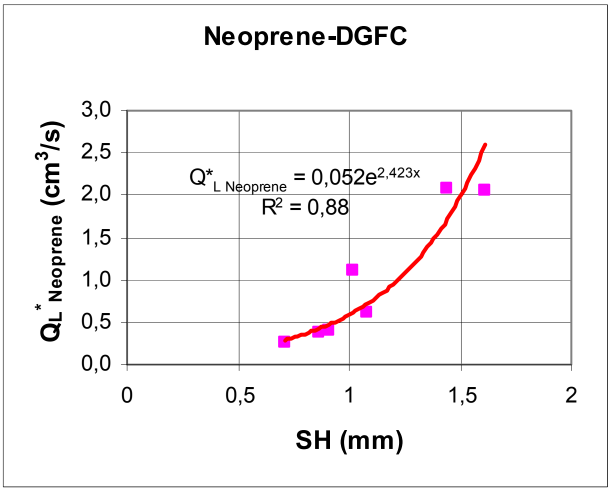

Figure 20: $Q^*_{LNeoprene}$ versus SH (DGFC)

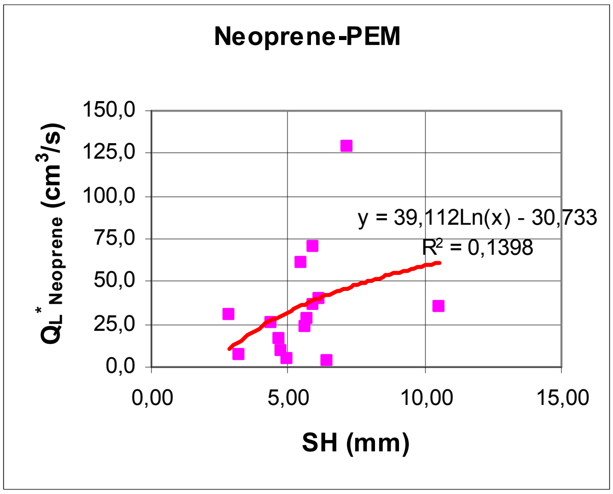

Figure 21: $Q^*_{LNeoprene}$ versus SH (PEM)

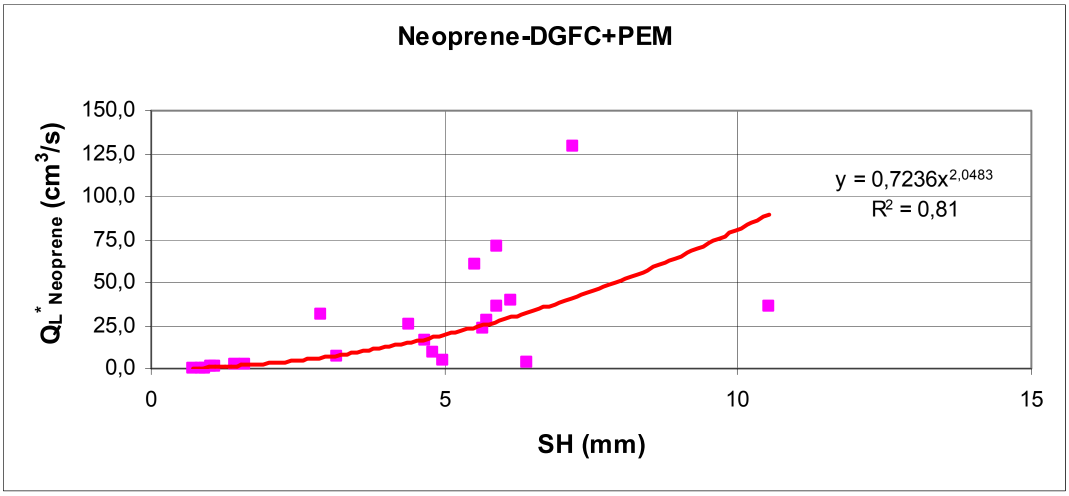

Figure 22: $Q^*_{LNeoprene}$ versus SH (DGFC+PEM)

When the standard case is analyzed (see figures 23 to 25, which refer to a base in cellular rubber SBR) the above discussed high variance of horizontal flow rates for high macro-texture values occurs again: R-square coefficients range from 0,45 (PEM) to 0,92 (DFGC).

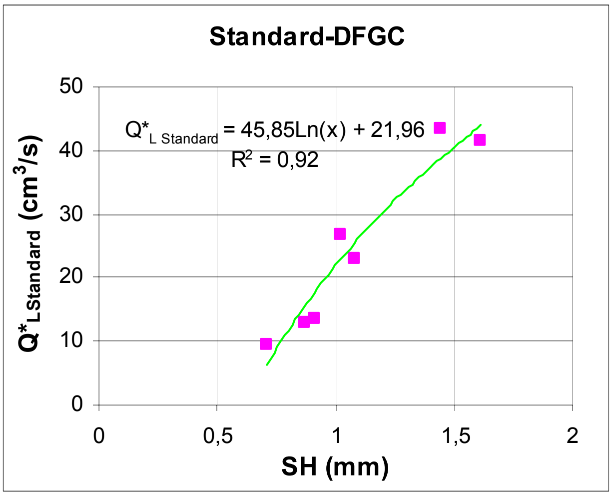

Figure 23: $Q^*_{LStandard}$ versus SH (DGFC)

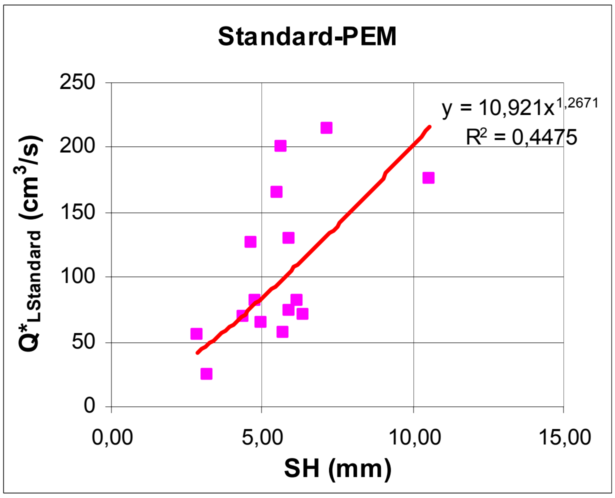

Figure 24: $Q^*_{LStandard}$ versus SH (PEM)

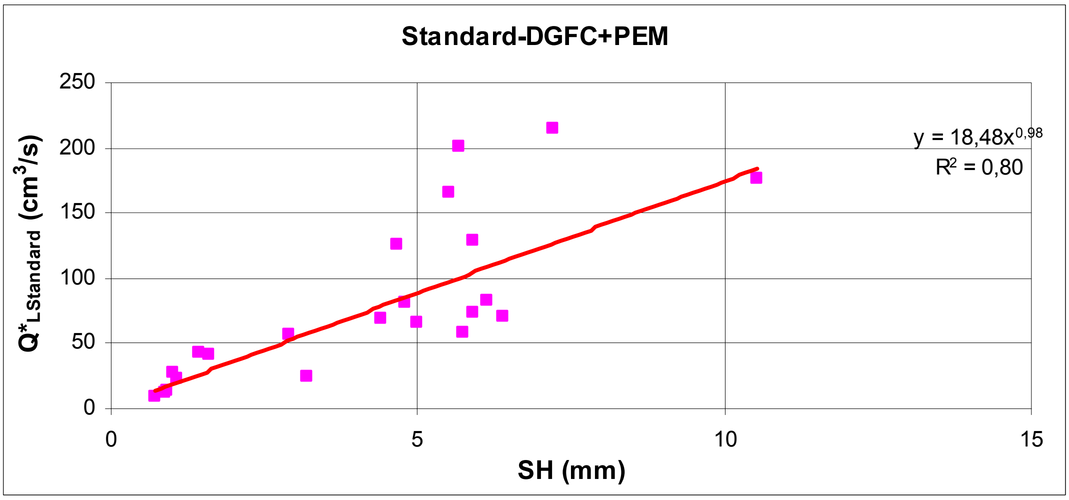

Figure 25: $Q^*_{LStandard}$ versus SH (DGFC+PEM)

Figures 26 to 28 show how the pavement macro-texture influences horizontal flows for the “None” case. As regards DGFCs, correlation is positive. The highest R-square coefficient is 0,97.

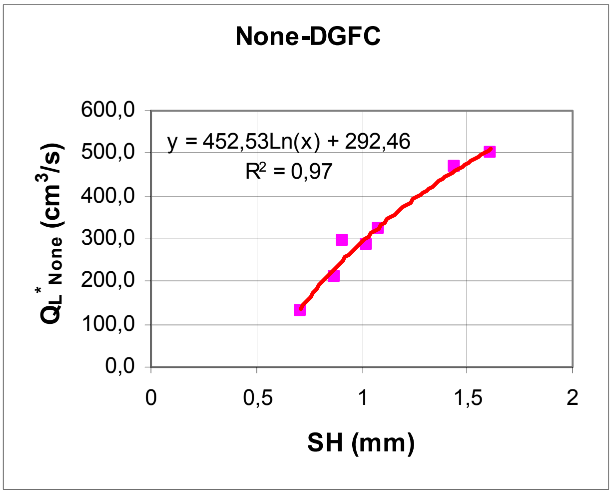

Figure 26: Q^*_{LNone} versus SH (DGFC)

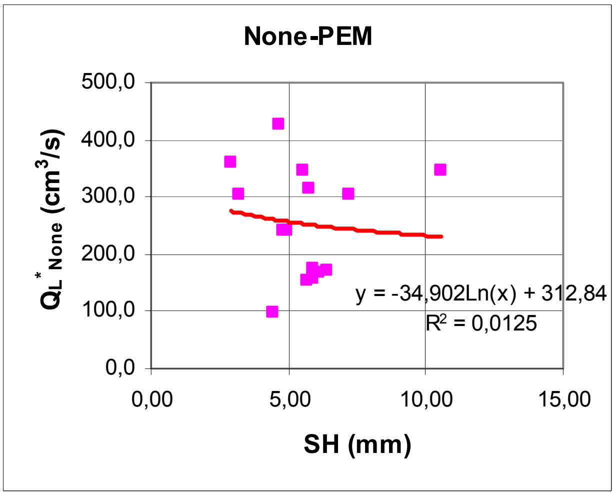

Figure 27: Q^*_{LNone} versus SH (PEM)

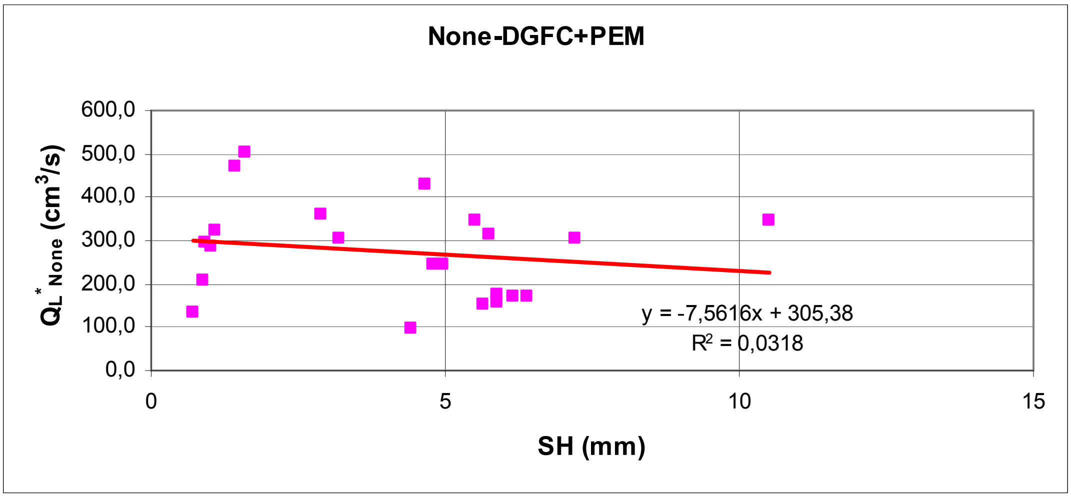

Figure 28: Q^*_{LNone} versus SH (DGFC+PEM)

By referring to Figure 27 and 28 one must observe that, for the case "None"-PEM, the measured outflow times were small (from 0,55s to 1,5s), in a range comparable with operator accuracy; this fact can contribute to explain the low R-square coefficients.

Figures 29 to 31 show the influence of macro-texture on the ratio $\left(\frac{Q^*_L}{Q_T}\right)$.

When pavements are separately examined, both for DGFC and for PEM R-square coefficients are low and the behavior quite not-defined.
Importantly, if one observes the overall behavior in Figure 31 curves interpolate quite well the three interesting boundary conditions.
One can suppose that, as SH increases, air voids effect on Q^*_F seem to prevail on macro-texture effect on Q^*_L.
For this case, correlations are negative and R-square coefficients range from 0,81 to 0,86. Importantly, in Figure 31, $\left(\frac{Q^*_L}{Q_T}\right)_{silicone}$, being zero, is not plotted.

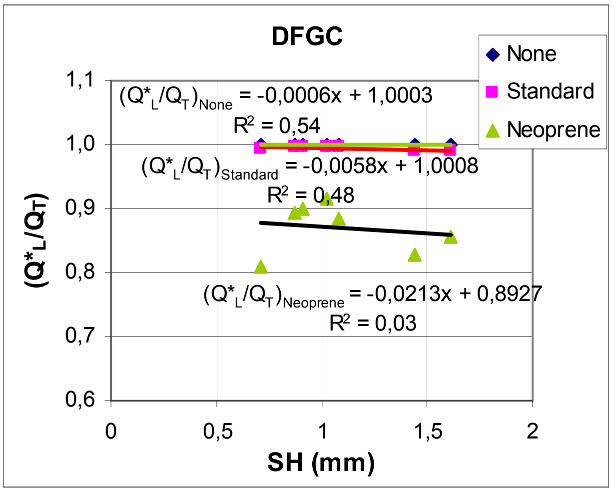

Figure 29: (Q^*_L/Q_T) versus SH (DGFC)

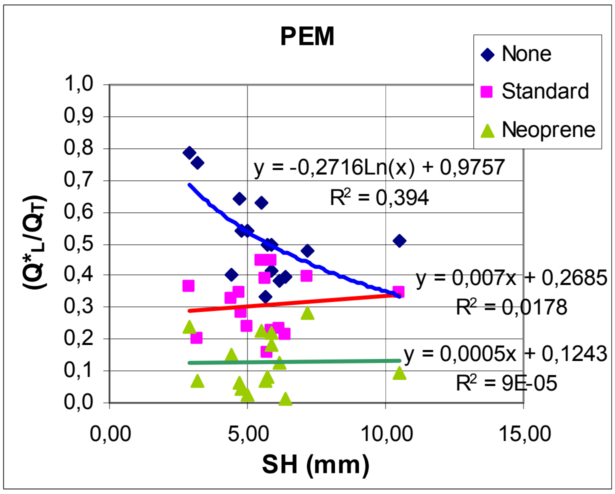

Figure 30: (Q^*_L/Q_T) versus SH (PEM)

Finally one can observe that with reference to the standard condition (that is to say by using the boundary conditions set out in Belgian standard) the ratio $\left(\frac{Q^*_L}{Q_T}\right)_{Standard}$ is equal to about 1 for DGFC and 0,3 for PEM.

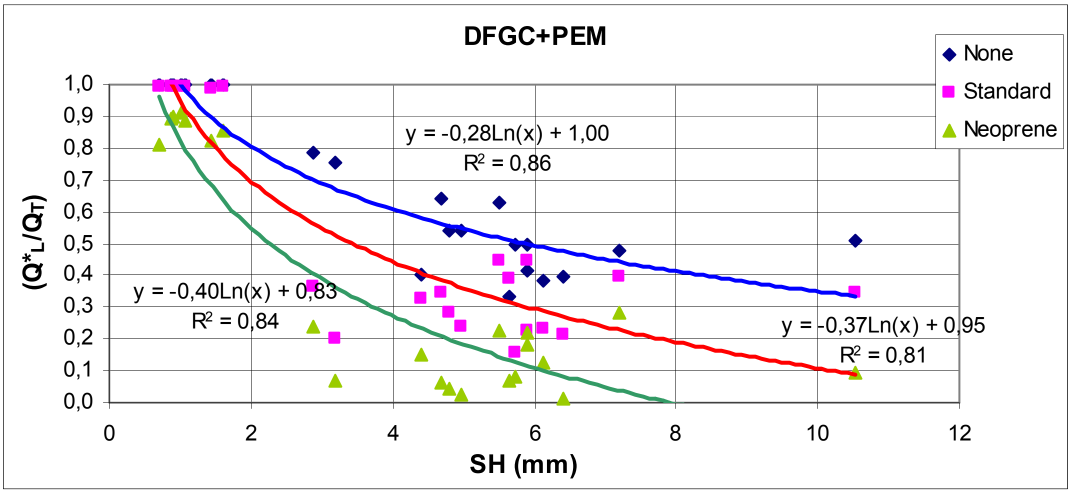

Figure 31: (Q^*_L/Q_T) versus SH (DGFC+PEM)

In first approximation, by observing again (Q^*_L/Q_T)j values in Table 6, this means that the effectiveness of the Belgian device in representing the concept of pavement (vertical) drainability increases as SH (and air voids) increases (towards low side of Figure 32) or/and "water-stop" boundary mechanism works better (towards right side, see Figure 32).

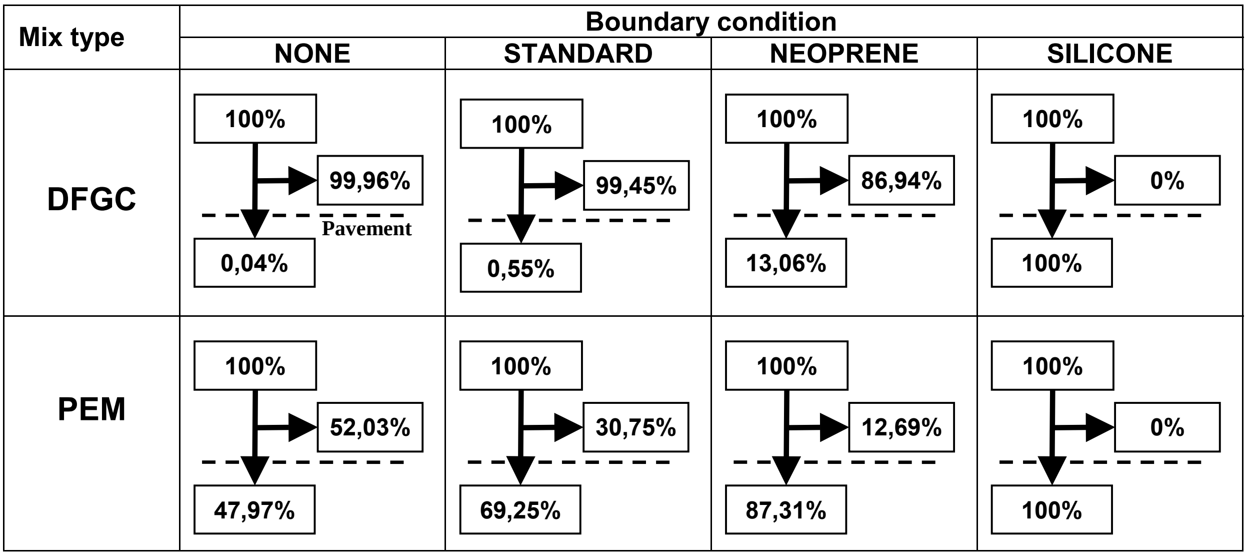

Mix type	Boundary condition			
	NONE	STANDARD	NEOPRENE	SILICONE
DFGC	100% 99,96% Pavement 0,04%	100% 99,45% 0,55%	100% 86,94% 13,06%	100% 0% 100%
PEM	100% 52,03% 47,97%	100% 30,75% 69,25%	100% 12,69% 87,31%	100% 0% 100%

Figure 32: Boundary conditions influence: a summary (average values)

Figure 33 shows how Δt times depend on hydraulic head. When the considered height increases 4 times (from 5 to 20 cm), the consequent time increases about five times (≈ +20%).

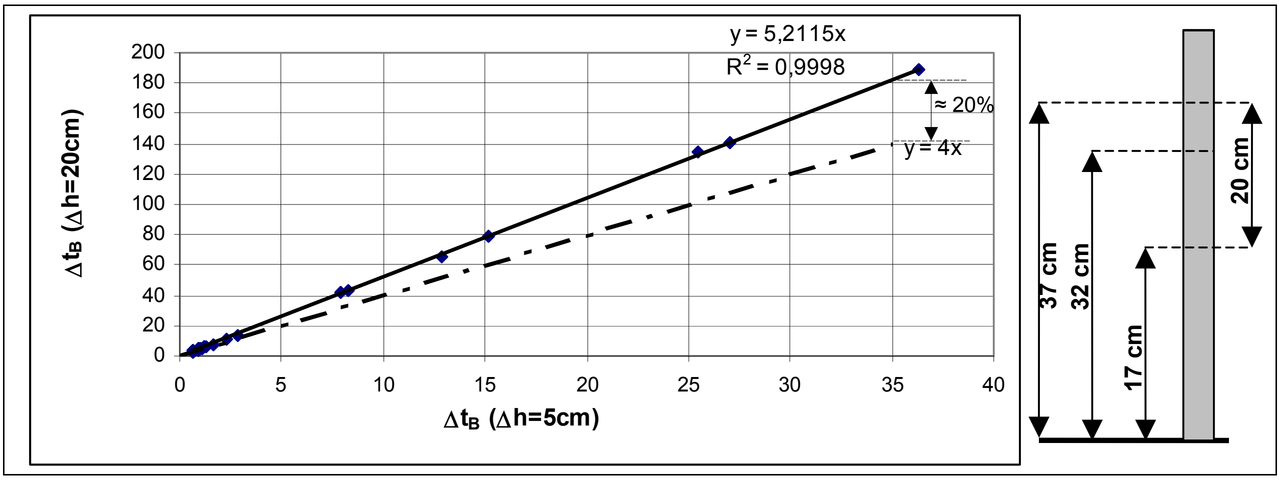

Figure 33: Influence of head on Δt_B

Finally, Figure 34 shows Δt behaviour when SH increases.

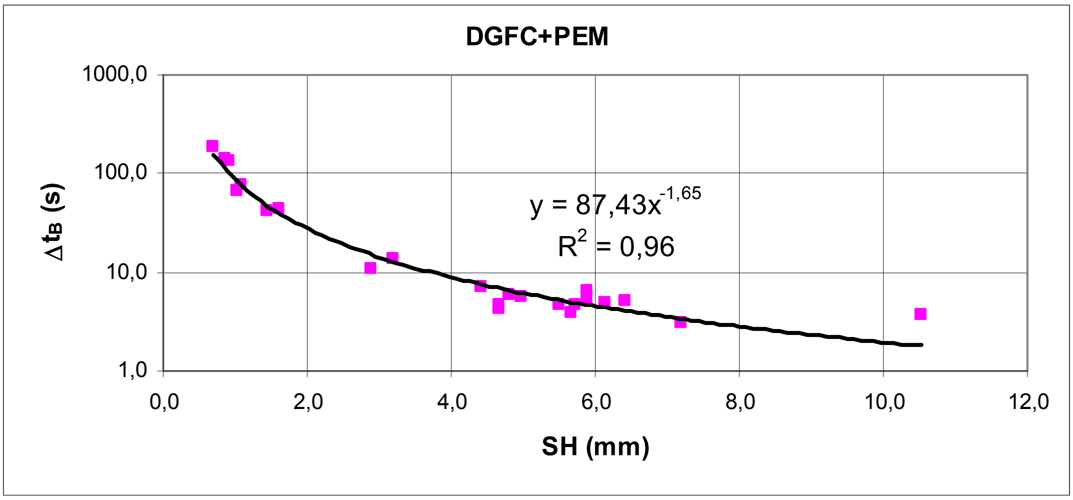

Figure 34: Δt$_B$ versus SH (PEM)

One can observe than if SH increases fifteen times, Δt decreases about sixty times. From a practical point of view, one can hypothesize that macro-texture, though representative of only surface properties (which control horizontal flow rates), being well correlated with bulk volumetrics (which control vertical flow rates), rules Δt values. R-square coefficient is 0.96 for the analysed cases. Significantly, one must observe that the aptitude of SH to be representative of also bulk properties is affected by the surface state of the HMA (wearing level). Therefore, the particular fitting curve obtained may be influenced also by this factor.

CONCLUSIONS

On the bases of the above studies and experiments, the following conclusions may be drown:
1) HMA outflow times are ruled by air voids and texture; their role may be considered, in general, more important than that of the remaining factors (thickness, etc.);
2) air voids and permeability have a peculiar influence on HMA mechanical properties;
3) The influence of the boundary conditions on drainability depends on both HMA volumetrics and surface properties;
4) macro-texture, though representative of only surface properties, being well correlated with bulk volumetrics, rules Δt values both for PEMs and DGFCs;
5) the effectiveness of the Belgian device in representing the concept of pavement (vertical) drainability increases as SH (and air voids) increases or/and "water-stop", boundary mechanism works better.

REFERENCES

ALLEN, D. L., SCHULTZ, D. B. Jr., FLECKENSTEIN, L. J. (2003), "Development and Proposed Implementation of a Field Permeability Test for Asphalt Concrete", Research Report KTC-01-19/SPR216-00-1F.

ALLEN, D. L., WANG, Y., SCHULTZ, D. B. Jr., FLECKENSTEIN, L. J. (2005), *Development of a New Field Permeability Test for Asphalt Concrete*, [CD-ROM], TRB Annual Meeting.

APUL, D. S. , GARDNER, K., EIGHMY, T., BENOIT, J., BRANNAKA, L. (2002), "A Review of Water Movement in the Highway Environment", Recycled Materials Resource Center Environmental Technology Building University of New Hampshire Durham, NH 03824.

ASTM PS 129-01 (2001), "Standard Provisional Test Method for Measurement of Permeability of Bituminous Paving Mixtures Using a Flexible Wall Permeameter".

AUSTROADS (1999), "Air Voids in Asphalt", *Pavement work tips*, no. 17.

BELLANGER, J., GEORGE L. (1999), "Cofiroute et l'UNGP testent un BBDr 0/6 depuis trois ans avec succés", *Revue générale des routes et des aérodromes*, n°770, pp. 39-42.

BRENGARTH, M., LAGANIER, R., BONNOT, J.(1983), "Drainoroute Mesure du pouvoir drainant de la texture d'une surface routière", *Bulletin des Laboratoires des Ponts et Chaussées*, 123, pp. 17-28.

BROSSEAUD, Y., ROCHE, J. (1997) "Chantier expérimental d'enrobés drainantes, bilan après huit annèes de trafic sur l'A 63", *Revue générale des routes et des aérodromes,* n°755, pp. 47-52.

CAFISO, S., DI FRANCO, M., DI GRAZIANO, A., TAORMINA, S.(2000), "Capacità drenante delle pavimentazioni in conglomerato bituminoso chiuso", X Convegno, SIIV,Catania.

CAROTI, L., LOSA, M. (1999), "La valutazione dei parametri fisici caratterizzanti il comportamento acustico e drenante dei conglomerati porosi", *Quarry & Construction*, pp. 99-108.

CASTELBLANCO, A., MASAD E., BIRGISSON B. (2005), *HMA Moisture Damage as a Function of Air Void Size Distribution, Pore Pressure and Bond Energy*, [CD-ROM], TRB 84th Annual Meeting, Washington.

CAVALIERE, M. G. (1997), "Il manto di usura drenante-fonoassorbente", *Strade & Autostrade*, n° 4, pp. 48-51.

CME - Chapitre 54, "Détermination de la drainabilité in situ d'enrobés drainants".

COOLEY, L. A., (1999), "Permeability of Superpave Mixtures: Evaluation of Field Permeameters", NCAT Report N. 99-1.

COOLEY, L. A., BROWN, E. R., WATSON D E.(2000), " Evaluation of OGFC Mixtures Containing Cellulose Fibers", NCAT Report N. 2000-05.

COOLEY, L. A., BROWN, E. R., MAGHSOODLOO, S. (2001), "Development of critical field permeability and pavement density values for Coarse-Graded Superpave Pavements", NCAT Report N. 01-03.

COOLEY, L. A., PROWELL, B. D., BROWN, E. R. (2002), "Issues Pertaining to the Permeability Characteristics of Coarse-Graded Superpave Mixes", NCAT Report N. 2002-06.

COOLEY, L. A.(2003), "Evaluation of Pavement Permeability in Mississippi", National Center for Asphalt Technology.

DE PALMA, C., BASSANI, M., (2000), "Manti d'usura fonoassorbenti realizzati con conglomerati bituminosi alleggeriti di tipo chiuso", *Strade & Autostrade*, n° 5, pp. 22-27.

DI BENEDETTO, H., JOUNI, M., HEURTEBISE, F. (1995), "Ecoulement dans le BBDr: le perméamètre VH", *Revue générale des routes et des aérodromes*, n°731, pp. 74-77.

DI BENEDETTO, H., JOUNI, M., HEURTEBISE, F. (1996a), "Ecoulement de solutions salines dans le BBDr", *Revue générale des routes et des aérodromes*, n°741, pp. 34-38.

DI BENEDETTO, H., JOUNI, M., BOILLON, P., SALHI, J. (1996b), "Mesures in situ et en laboratoire des écoulement dans les BBDr, modélisation et validation", *Bulletin des Laboratoires des Ponts et Chaussées*, 204, pp. 3-13.

FAGHRI, M., SADD, M H., CARDIN, J., DALY, P., PARK, K., TANAKA, C., GONCALVES, E. (2002), "Performance Improvement of Open-Graded Asphalt Mixes", URITC PROJECT N. 536144.

FM 5-565 (2004), "Florida Method of Test For Measurement of Water Permeability of Compacted Asphalt Paving Mixtures", Florida Department of Transportation.

GEORGIA, "Georgia Department of Transportation's Progress in Open-Graded Friction Course Development", Transportation Research Record 1616.

GOGULA, A., HOSSAIN, M., ROMANOSCHI, S., FAGER, G. A. (2003), "Correlation between the Laboratory and Field Permeability Values for the Superpave Pavements", Proceedings of the 2003 Mid-Continent Transportation Research Symposium.

HARVEY, J. T., DEACON, J. A., TSAI, B., MONISMITH, C. L. (1995), "Fatigue Performance of Asphalt Concrete Mixes and its Relationship to Asphalt Concrete Pavement Performance in California", Report RTA-65W485-2.

HUNTER, E. R., KSAIBATI, K. (2001), "Evaluating Moisture Susceptibility of Asphalt Mixes", Department Civil and Architectural Engineering University of Wyoming P.O. Box 3295 Laramie, WY 82071-3295.

JIMÉNEZ PÉREZ, F. E., CALZADA PÉREZ, M. A. (1990), "Analysis and Evaluation of the Performance of Porous Asphalt : The Spanish Experience", ASTM STP 1031.

KANDHAL, P S.(1990), "Design of large Stone Asphalt Mixes to minimize Rutting", NCAT Report N. 90-1.

KANDHAL, P. S., CROSS, S. A., BROWN, E. R. (1993), "Heavy Duty Asphalt Pavements in Pennsylvania: an Evaluation for Rutting", NCAT Report N. 93-2.

KANDHAL, P. S., RAO, S. S., WATSON D. E., YOUNG B. (1995), "Performance of Recycled Hot Mix Asphalt Mixtures", NCAT Report N. 95-1.

KANDHAL, P. S., CHAKRABORTY, S. (1996), "Evaluation of Voids in the Mineral Aggregate for HMA Paving Mixtures", NCAT Report N. 96-4.

KANDHAL, P. S., MALLICK, R. B., BROWN, E. R. (1998), "Hot Mix Asphalt for Intersections in Hot Climates ", NCAT Report N. 98-6.

KANDHAL, P. S., MALLICK, R. B. (1999), "Design of New-Generation Open-Graded Friction courses", NCAT Report N_0. 99-3.

KANITPONG, K., BAHIA, H., RUSSELL, J., SCHMITT R. (2005), *Predicting Field Permeability from Testing HMA Specimens Produced by the Superpave Gyratory Compactor*, [CD-ROM], TRB 84th Annual Meeting, Washington.

KENNEDY, T. W., COMINSKY, R. J., HARRIGAN, E. T., LEAHY, R. B.(1990), "Hypotheses and Models Employed in the SHRP Asphalt Research Program", SHRP-A/WP-90-008.

LAUREN (2005), "A Reference Guide To Design and Implementation of Extruded Polymer Products", 2228 Reiser Ave. S.E. New Philadelphia, Ohio 44663.

MAHER, A., BENNERT, T., WALKER III, L A.(2001), " Evaluation of a Rutting/Fatigue Cracking Device", FHWA-NJ-2001-031.

MALLICK, R. B., KANDHAL, P. S., COOLEY, L. A., WATSON D. E., (2000) "Design, Construction, and Performance of New-Generation Open-Graded Friction courses", NCAT Report N. 2000-01.

MALLICK, R. B., COOLEY, L. A., TETO, M., BRADBURY, R. L. (2001), "Development of A Simple Test for Evaluation of In-Place Permeability of Asphalt Mixes", *International Journal of Pavement Engineering*.

MALLICK, R. B., COOLEY, L. A., TETO, M., BRADBURY, R. L., PEABODY, D. (2001), "An Evaluation of Factors Affecting Permeability of Superpave Designed Pavements", NCAT Report 03-02.

MASCHIETTO, M. (1995), "Drenante come nuovo", *Le Strade*, n° 9, pp. 683-686.

MAUPIN, G. W. (2000), "Investigation of Test Methods, Pavements, and Laboratory Design Related to Asphalt Permeability", Final Report, Virginia Transportation Research Council.

MAUPIN, G. W. (2005), *Asphalt Mix Design Method for Permeability*, [CD-ROM], TRB Annual Meeting.

MOGAWER, W. S., MALLICK, R. B., TETO, M., CROCKFORD, W. C. (2002), "Evaluation of Permeability of Superpave Mixes", Project No. NETC 00-2.

MURALI KRISHNAN, J., LAKSHMANA RAO, C. (2001), "Permeability and bleeding of asphalt concrete using mixture theory", *International Journal of Engineering Science*, Volume 39, pp. 611-627.

NCHRP (2002a), "Recommended Performance-Related Specification for Hot-Mix Asphalt Construction: Results of WesTrack Project", Materials Characterization and Performance Models, Chapter 5, Report 455, TRB.

NCHRP (2002b), "Significance of "As-Constructed" HMA Air Voids to Pavement Performance from an Analysis of LTPP Data", Research Results Digest, TRB.

NCHRP (2004), "Relationships of HMA In-Place Air Voids, Lift Thickness, and Permeability", Project 9-27, TRB.

NCHRP (2005), "Performance and Maintenance of Permeable Friction Courses", Project 9-41.

OKLAHOMA D.O.T.(2004), "OHD L-44 Method of Test For Measurement of Water Permeability of Compacted Paving Mixtures".

OLIVEIRA, C. G. M., (2003), "Estudo de Propriedades Mecânicas e Hidráulicas do Concreto Asfáltico Drenante", Dissertação de Mestrado, G. DM – 111A/03, Brasília.

PARIAT, J., AVERSENQ, B.(1992), "Suivi du décolmatage d'enrobés drainants en bande d'arret d'urgence et voie lente d'autoroute", *Bulletin des Laboratoires des Ponts et Chaussées*, 179, pp. 3-9.

PELLAND, R. J., GOULD, J. G., MALLICK, R. B.,(2003) "Selecting a Rut Resistant Hot Mix Asphalt for Boston-Logan International Airport", in *Airfield Pavements: Challenges and New Technologies, Conference Proceeding*, Las Vegas, Nevada, Moses Karakouzian (editor).

POULIKAKOS, L. D., TAKAHASHI, S., PARTL, M. N. (2004), "A Comparison of Swiss and Japanese Porous Asphalt Through Various Mechanical Tests", in *Swiss Transport Research Conference*, Ascona.

PRATICO', F. G., MORO A. (2005), "Sulla permeabilità dei conglomerati bituminosi: strumentazioni, modellistica e sperimentazioni", *Strade & Autostrade*, n°1, pp. 68-79.

PROWELL, B D. (2000), "Design, Construction, and Early performance of Hot-Mix Asphalt Stabilizer and Modifier Test Sections", Virginia Transportation Research Council.

PROWELL, B D. (2001), "Technical Assistance Report Investigation of Pavement Permeability: Old Bridge Road", Virginia Transportation Research Council.

VIRGINIA TEST METHODS – 120 (2003), "Method of Test For Measurement of Permeability of Bituminous Paving Mixtures Using a Flexible Wall Permeameter".

WOLTERS, R. O.(2003), "Raveling of Hot-Mix-Asphalt", Minnesota Asphalt Pavement Association.

APPENDICES

Tab 2: Review of HMA permeability and outflow times literature

PAPER	PAVEMENT TYPE	AIR VOIDS (%)	THICKNESS RANGE (cm)	NMAS (mm)	COMPACTION PROCEDURE	DEVICE	INDICATOR	FLUID	INDICATOR RANGE
(NCHRP, 2004)	Fine-Graded	6,5 ÷ 8,8	2,1 ÷ 5,8	9,5	SR	NCAT	k (cm/sec · 10^{-5})	H_2O	1 ÷ 28
	Fine-Graded	6,5 ÷ 8,8	2,1 ÷ 5,8	9,5	SR	FWP (PS 129)	k_V (cm/sec · 10^{-5})	H_2O	1 ÷ 35
	Coarse-Graded	9 ÷ 12	2,0 ÷ 5,4	9,5	SWR	NCAT	k (cm/sec · 10^{-5})	H_2O	22 ÷ 532
	Coarse-Graded	9÷12	2,0 ÷ 5,4	9,5	SWR	FWP (PS 129)	k_V (cm/sec · 10^{-5})	H_2O	234 ÷ 871
	Coarse-Graded	9,7 ÷ 13	1,87 ÷ 4,9	9,5	SRT	NCAT	k (cm/sec · 10^{-5})	H_2O	14 ÷ 632
	Coarse-Graded	9,7 ÷ 13	1,87 ÷ 4,9	9,5	SRT	FWP (PS 129)	k_V (cm/sec · 10^{-5})	H_2O	107 ÷ 1070
	SMA	7,7 ÷ 13	2,10 ÷ 5,2	9,5	SWR	NCAT	k (cm/sec · 10^{-5})	H_2O	110 ÷ 379
	SMA	7,7 ÷ 13	2,10 ÷ 5,2	9,5	SWR	FWP (PS 129)	k_V (cm/sec · 10^{-5})	H_2O	29 ÷ 124
	SMA	8,8 ÷ 11	2,00 ÷ 5,0	9,5	SRT	NCAT	k (cm/sec · 10^{-5})	H_2O	135 ÷ 651
	SMA	8,8 ÷ 11	2,00 ÷ 5,0	9,5	SRT	FWP (PS 129)	k_V (cm/sec · 10^{-5})	H_2O	19 ÷ 168
	SMA	4,1 ÷ 18	2,50 ÷ 6,5	12,5	SR	NCAT	k (cm/sec · 10^{-5})	H_2O	6 ÷ 1455
	SMA	4,1 ÷ 18	2,50 ÷ 6,5	12,5	SR	FWP (PS 129)	k_V (cm/sec · 10^{-5})	H_2O	0,1 ÷ 2807
	SMA	7,0 ÷ 16	2,53 ÷ 6,4	12,5	SRT	NCAT	k (cm/sec · 10^{-5})	H_2O	50 ÷ 1965
	SMA	7,0 ÷ 16	2,53 ÷ 6,4	12,5	SRT	FWP (PS 129)	k_V (cm/sec · 10^{-5})	H_2O	113 ÷ 5850
	Fine-Graded	5,7 ÷ 9,5	3,80 ÷ 9,8	19	SR	NCAT	k (cm/sec · 10^{-5})	H_2O	38 ÷ 161
	Fine-Graded	5,7 ÷ 10	3,80 ÷ 9,8	19	SR	FWP (PS 129)	k_V (cm/sec · 10^{-5})	H_2O	1 ÷ 77
	Coarse-Graded	5,5 ÷ 9,8	4,00 ÷ 9,6	19	SR	NCAT	k (cm/sec · 10^{-5})	H_2O	33 ÷ 1760
	Coarse-Graded	5,5 ÷ 9,8	4,00 ÷ 9,6	19	SR	FWP (PS 129)	k_V (cm/sec · 10^{-5})	H_2O	33 ÷ 141
	Coarse-Graded	1 ÷ 14	4,00 ÷ 9,2	19	SRT	NCAT	k (cm/sec · 10^{-5})	H_2O	10 ÷ 1057
	Coarse-Graded	1 ÷ 14	4,00 ÷ 9,2	19	SRT	FWP (PS 129)	k_V (cm/sec · 10^{-5})	H_2O	1 ÷14
	Coarse-Graded M	5,4 ÷ 12	3,73 ÷ 9,97	19	SWR	NCAT	k (cm/sec · 10^{-5})	H_2O	72 ÷ 1030
	Coarse-Graded M	5,4 ÷ 12	3,73 ÷ 9,97	19	SWR	FWP (PS 129)	k_V (cm/sec · 10^{-5})	H_2O	0 ÷ 1203
	Coarse-Graded M	6,9 ÷ 15	3,63 ÷ 11,6	19	SRT	NCAT	k (cm/sec · 10^{-5})	H_2O	611 ÷ 3030
	Coarse-Graded M	6,9 ÷ 15	3,63 ÷ 11,6	19	SRT	FWP (PS 129)	k_V (cm/sec · 10^{-5})	H_2O	0 ÷ 304
	ARZ	6,2 ÷ 6,8	3,77 ÷ 3,81	9,5	SGC	FWP (PS 129)	k_V (cm/sec · 10^{-5})	H_2O	1 ÷ 4
	ARZ	6,1 ÷ 8	3,96 ÷ 7,57	19	SGC	FWP (PS 129)	k_V (cm/sec · 10^{-5})	H_2O	0 ÷ 117
	BRZ	6,8 ÷ 7,7	3,75 ÷ 3,98	9,5	SGC	FWP (PS 129)	k_V (cm/sec · 10^{-5})	H_2O	7 ÷ 40
	BRZ	6,1 ÷ 7,7	5,70 ÷ 7,74	19	SGC	FWP (PS 129)	k_V (cm/sec · 10^{-5})	H_2O	21 ÷ 303
	SMA	6,5 ÷ 7,7	7,67 ÷ 7,78	19	SGC	FWP (PS 129)	k_V (cm/sec · 10^{-5})	H_2O	2 ÷ 559
	ARZ	6 ÷ 8	1,90 ÷ 3,95	9,5	SVC	FWP (PS 129)	k_V (cm/sec · 10^{-5})	H_2O	1 ÷ 32
	ARZ	6,2 ÷ 8	3,90 ÷ 7,50	19	SVC	FWP (PS 129)	k_V (cm/sec · 10^{-5})	H_2O	0 ÷ 47
	BRZ	6,4 ÷ 8	1,81 ÷ 3,98	9,5	SVC	FWP (PS 129)	k_V (cm/sec · 10^{-5})	H_2O	0 ÷ 122
	BRZ	6 ÷ 7,9	3,82 ÷ 7,56	19	SVC	FWP (PS 129)	k_V (cm/sec · 10^{-5})	H_2O	0 ÷ 174
	SMA	6 ÷ 7,8	1,80 ÷ 3,95	9,5	SVC	FWP (PS 129)	k_V (cm/sec · 10^{-5})	H_2O	0 ÷ 301
	SMA	6 ÷ 7,8	2,43 ÷ 5,15	12,5	SVC	FWP (PS 129)	k_V (cm/sec · 10^{-5})	H_2O	0 ÷ 470
	SMA	6 ÷ 8	3,68 ÷ 7,7	19	SVC	FWP (PS 129)	k_V (cm/sec · 10^{-5})	H_2O	0 ÷ 49
(MALLICK et al., 2001) (MALLICK et al., 2003)	Fine-Graded	5,8 ÷ 12	4,00	9,5		WPIP	k (cm/sec · 10^{-5})	H_2O	12 ÷ 634
	Fine-Graded	5,8 ÷ 12	4,00	9,5	cores	FWP(FM5-565)	k_V (cm/sec · 10^{-5})	H_2O	27 ÷ 980
	Coarse-Graded	2,9 ÷ 8,1	3,00	9,5		WPIP	k (cm/sec · 10^{-5})	H_2O	0,63 ÷ 100
	Coarse-Graded	2,9 ÷ 8,1	3,00	9,5	cores	FWP(FM5-565)	k_V (cm/sec · 10^{-5})	H_2O	0 ÷ 187
	Coarse-Graded	2,2 ÷ 8,4	4,00	12,5		WPIP	k (cm/sec · 10^{-5})	H_2O	0,94 ÷ 655
	Coarse-Graded	2,2 ÷ 8,4	4,00	12,5	cores	FWP(FM5-565)	k_V (cm/sec · 10^{-5})	H_2O	0 ÷ 659
	Coarse-Graded	5,8 ÷ 8,4	5,00	19		WPIP	k (cm/sec · 10^{-5})	H_2O	59,81 ÷ 2362
	Coarse-Graded	5,8 ÷ 8,4	5,00	19	cores	FWP(FM5-565)	k_V (cm/sec · 10^{-5})	H_2O	21 ÷ 676
	Coarse-Graded	4,5 ÷ 9,2	8,9	25		WPIP	k (cm/sec · 10^{-5})	H_2O	596 ÷ 12263
	Coarse-Graded	4,5 ÷ 9,2	8,9	25	cores	FWP(FM5-565)	k_V (cm/sec · 10^{-5})	H_2O	0 ÷ 98
(MALLICK et al., 2000) (KANDHAL et al., 1999) (COOLEY et al., 2000)	OGFC	13 ÷ 15			SGC	FWP(FM5-565)	k_V (cm/sec · 10^{-5})	H_2O	2400 ÷ 13500
	OGFC	16,7 (Avg.)			cores	FWP(FM5-565)	k_V (cm/sec · 10^{-5})	H_2O	852 ÷ 4358
	OGFC (Cr. rubber)	15,8 (Avg.)			cores	FWP(FM5-565)	k_V (cm/sec · 10^{-5})	H_2O	538 ÷ 10620
	OGFC (Min. fibers)	19,9 (Avg.)			cores	FWP(FM5-565)	k_V (cm/sec · 10^{-5})	H_2O	257 ÷ 8402
	OGFC (Cell. fibers)	16,2 (Avg.)			cores	FWP(FM5-565)	k_V (cm/sec · 10^{-5})	H_2O	350 ÷ 15249
	OGFC (SB Polym.)	13,9 (Avg.)			cores	FWP(FM5-565)	k_V (cm/sec · 10^{-5})	H_2O	874 ÷ 3525
	OGFC(SB+Cel.Fib.)	19,2 (Avg.)			cores	FWP(FM5-565)	k_V (cm/sec · 10^{-5})	H_2O	687 ÷ 18582
(GOGULA et al., 2003)	Superpave Mixes	3,6 ÷ 4,7		19		NCAT	k (cm/sec · 10^{-5})	H_2O	164 ÷ 1300
	Superpave Mixes	5,5 ÷ 9,0		19	SGC		k_V (cm/sec · 10^{-5})	H_2O	0,33 ÷ 10,84
	Superpave Mixes	3,3 ÷ 4,7		12,5		NCAT	k (cm/sec · 10^{-5})	H_2O	364 ÷ 700
	Superpave Mixes	5,0 ÷ 6,9		12,5	SGC		k_V (cm/sec · 10^{-5})	H_2O	0,29 ÷ 2,5

Tab 2: Review of HMA permeability and outflow times literature - continued

PAPER	PAVEMENT TYPE	AIR VOIDS (%)	THICKNESS RANGE (cm)	NMAS (mm)	COMPACTION PROCEDURE	DEVICE	INDICATOR	FLUID	INDICATOR RANGE
(FAGHRI et al., 2002)	OGFC (Non-mod.)	13,0 ÷ 18,4				FHT	$k_{V.}$ (cm/sec · 10^{-5})	H_2O	4370 ÷ 45320
	OGFC (Fiber)	12,6 ÷ 18,1				FHT	$k_{V.}$ (cm/sec · 10^{-5})	H_2O	440 ÷ 25720
	OGFC (SBS)	14,0 ÷ 17,1				FHT	$k_{V.}$ (cm/sec · 10^{-5})	H_2O	7400 ÷ 4638
	OGFC (Fib.+SBS)	12,9 ÷ 18,6				FHT	$k_{V.}$ (cm/sec · 10^{-5})	H_2O	9380 ÷ 36510
(MAUPIN , 2000)	Superpave Mixes	7,7 ÷ 10,6	3,5 ÷ 4,0	9,5	cores	FWP (PS 129)	$k_{V.}$ (cm/sec · 10^{-5})	H_2O	1,6 ÷ 380
	Superpave Mixes	4,5 ÷ 13,6	3,5 ÷ 4,0	12,5	cores	FWP (PS 129)	$k_{V.}$ (cm/sec · 10^{-5})	H_2O	10 ÷ 600
	Superpave Mixes	5,8 ÷ 10,6	3,5 ÷ 4,0	19	cores	FWP (PS 129)	$k_{V.}$ (cm/sec · 10^{-5})	H_2O	10 ÷ 700
	Superpave Mixes	4,2 ÷ 9,3	3,5 ÷ 4,0	25	cores	FWP (PS 129)	$k_{V.}$ (cm/sec · 10^{-5})	H_2O	10 ÷ 2000
	SMA	6,3 ÷ 11,7	3,5 ÷ 4,0		cores	FWP (PS 129)	$k_{V.}$ (cm/sec · 10^{-5})	H_2O	7 ÷ 4000
	SM-2	7,4 ÷ 19,2	3,5 ÷ 4,0		cores	FWP (PS 129)	$k_{V.}$ (cm/sec · 10^{-5})	H_2O	20 ÷ 5000
(COOLEY et al., 2001)	Coarse-Graded	3,1 ÷ 13,6		9,5		NCAT	k (cm/sec · 10^{-5})	H_2O	1 ÷ 1200
	Coarse-Graded	2,3 ÷ 12,0		12,5		NCAT	k (cm/sec · 10^{-5})	H_2O	1 ÷ 1160
	Coarse-Graded	4,6 ÷ 10,8		19		NCAT	k (cm/sec · 10^{-5})	H_2O	20 ÷ 2000
	Coarse-Graded	4,1 ÷ 8,6		25		NCAT	k (cm/sec · 10^{-5})	H_2O	60 ÷ 1920
	Coarse-Graded			9,5			$K_{crit.}$ (cm/sec · 10^{-5})	H_2O	100
	Coarse-Graded			12,5			$K_{crit.}$ (cm/sec · 10^{-5})	H_2O	100
	Coarse-Graded			19			$K_{crit.}$ (cm/sec · 10^{-5})	H_2O	120
	Coarse-Graded			25			$K_{crit.}$ (cm/sec · 10^{-5})	H_2O	150
(COOLEY, 2003)	Fine-Graded	3,8 ÷ 13,9	3,30 ÷ 6,9	12,5		NCAT	k (cm/sec · 10^{-5})	H_2O	1 ÷ 697
	Coarse-Graded	3,7 ÷ 15,1	2,80 ÷ 6,1	9,5		NCAT	k (cm/sec · 10^{-5})	H_2O	28 ÷ 2345
	Coarse-Graded	3,9 ÷ 15,0		12,5		NCAT	k (cm/sec · 10^{-5})	H_2O	1 ÷ 2503
	Coarse-Graded	4,1 ÷ 13,1	3,10 ÷ 9,8	19		NCAT	k (cm/sec · 10^{-5})	H_2O	1 ÷ 17789
(PROWELL, 2001)	Superpave Mixes	8,2 ÷ 17,0	4,30 ÷ 6,9	12,5		NCAT	k (cm/sec · 10^{-5})	H_2O	17 ÷ 842
	Superpave Mixes	7,0 ÷ 17,0	4,30 ÷ 6,9	12,5		FWP (PS 129)	k (cm/sec · 10^{-5})	H_2O	20 ÷ 5550
(KANITPONG et al., 2005]	Coarse-Graded			12,5-19		NCAT	k (cm/sec · 10^{-5})	H_2O	70 ÷ 11500
	Fine-Graded			9,5-19-25		NCAT	k (cm/sec · 10^{-5})	H_2O	5 ÷ 2750
	Coarse-Graded			12,5-19	cores	FWP(D5084)	$k_{V.}$ (cm/sec · 10^{-5})	H_2O	1 ÷ 105
	Fine-Graded			9,5-19-25	cores	FWP(D5084)	$k_{V.}$ (cm/sec · 10^{-5})	H_2O	0 ÷ 110
(MAUPIN , 2005)	Superpave Mixes	4,6 ÷ 10,6	3,80	9,5	cores	FWP (PS 129)	$k_{V.}$ (cm/sec · 10^{-5})	H_2O	1 ÷ 1000
	Superpave Mixes	6,6 ÷ 12,3	3,80	12,5	cores	FWP (PS 129)	$k_{V.}$ (cm/sec · 10^{-5})	H_2O	3 ÷ 4800
	Superpave Mixes	6,6 ÷ 11,1	3,80	9,5	SGC	FWP (PS 129)	$k_{V.}$ (cm/sec · 10^{-5})	H_2O	3,5 ÷ 1000
	Superpave Mixes	6,7 ÷ 11,8	3,80	12,5	SGC	FWP (PS 129)	$k_{V.}$ (cm/sec · 10^{-5})	H_2O	3 ÷ 1000
(COOLEY et al., 2002)	Coarse-Graded	3,0 ÷ 16,0	3,80 ÷ 4,0	9,5		NCAT	k (cm/sec · 10^{-5})	H_2O	0 ÷ 3000
	Coarse-Graded	2,3 ÷ 15,0	3,80 ÷ 6,4	12,5		NCAT	k (cm/sec · 10^{-5})	H_2O	0 ÷ 2500
	Coarse-Graded	4,0 ÷ 11,0	5,00 ÷ 7,5	19		NCAT	k (cm/sec · 10^{-5})	H_2O	0 ÷ 3300
	Coarse-Graded	4,0 ÷ 8,5	5,00 ÷ 7,5	25		NCAT	k (cm/sec · 10^{-5})	H_2O	70 ÷ 3650
	SMA	4,6 ÷ 10,6	3,80	9,5		NCAT	k (cm/sec · 10^{-5})	H_2O	40 ÷ 1500
	Coarse-Graded	3,0 ÷ 15,3	3,80 ÷ 4,0	9,5	cores	FWP	$k_{V.}$ (cm/sec · 10^{-5})	H_2O	0 ÷ 2700
	Coarse-Graded	2,3 ÷ 14,0	3,80 ÷ 6,4	12,5	cores	FWP	$k_{V.}$ (cm/sec · 10^{-5})	H_2O	0 ÷ 2800
	Coarse-Graded	5,0 ÷ 10,6	5,00 ÷ 7,5	19	cores	FWP	$k_{V.}$ (cm/sec · 10^{-5})	H_2O	15 ÷ 2700
	Coarse-Graded	6,0 ÷ 10,6	5,00	9,5	SGC	FWP	$k_{V.}$ (cm/sec · 10^{-5})	H_2O	0 ÷ 450
	Coarse-Graded	5,3 ÷ 11,4	5,00	12,5	SGC	FWP	$k_{V.}$ (cm/sec · 10^{-5})	H_2O	0 ÷ 1500
	Coarse-Graded	7,0 ÷ 10,5	5,00	19	SGC	FWP	$k_{V.}$ (cm/sec · 10^{-5})	H_2O	15 ÷ 1050
(COOLEY, 1999)	Superpave Mixes			9		NCAT	k (cm/sec · 10^{-5})	H_2O	11 ÷ 15263
	Superpave Mixes				cores	FWP	$k_{V.}$ (cm/sec · 10^{-5})	H_2O	120 ÷ 5420
(ALLEN et al., 2003) (ALLEN et al., 2005)	0.38” Surface					AIP	V (mm Hg)	air	8,5 ÷ 495,7
	0.38” Surface				cores	FWP	$k_{V.}$ (cm/sec · 10^{-5})	H_2O	1,1 ÷ 4321
	0.5” Surface					AIP	V (mm Hg)	air	5,1 ÷ 561,4
	0.5” Surface				cores	FWP	$k_{V.}$ (cm/sec · 10^{-5})	H_2O	0,1 ÷ 16400
	0.5” Surface					NCAT	k (cm/sec · 10^{-5})	H_2O	1,3 ÷ 5619
	0.75” Base					AIP	V (mm Hg)	air	0,8 ÷ 574,3
	0.75” Base					NCAT	k (cm/sec · 10^{-5})	H_2O	5,6 ÷ 2800
	1.0”/1.5” Base					AIP	V (mm Hg)	air	5,3 ÷ 408,5
	1.0”/1.5” Base					NCAT	k (cm/sec · 10^{-5})	H_2O	0 ÷ 8856
	1.0”/1.5” Base				cores	FWP	$k_{V.}$ (cm/sec · 10^{-5})	H_2O	6,3 ÷ 10623
(MOGAWER et al., 2002)	Superpave Mixes	4,4 ÷ 11,5		9,5	SGC	FWP(FM5-565)	$k_{V.}$ (cm/sec · 10^{-5})	H_2O	10,5 ÷ 683
	Superpave Mixes	4,4 ÷ 13,2		12,5	SGC	FWP(FM5-565)	$k_{V.}$ (cm/sec · 10^{-5})	H_2O	3,65 ÷ 2610
	Superpave Mixes	4,9 ÷ 12,4		19	SGC	FWP(FM5-565)	$k_{V.}$ (cm/sec · 10^{-5})	H_2O	31,8 ÷ 3150

Tab 2: Review of HMA permeability and outflow times literature - continued

PAPER	PAVEMENT TYPE	AIR VOIDS (%)	THICKNESS RANGE (cm)	NMAS (mm)	COMPACTION PROCEDURE	DEVICE	INDICATOR	FLUID	INDICATOR RANGE
(DI BENEDETTO et al., 1995)	Enrobés Drainants	22,1	4,25		cores (slab)	VH	k_V (cm/sec · 10^{-5} a 5°C)	H_2O	72050 ÷ 74100
	Enrobés Drainants	22,1	4,25		cores (slab)	VH	k_V (cm/sec · 10^{-5} a 10°C)	H_2O	81100 ÷ 82350
	Enrobés Drainants	22,1	4,25		cores (slab)	VH	k_V (cm/sec · 10^{-5} a 15°C)	H_2O	94100 ÷ 95800
	Enrobés Drainants	22,1	4,25		cores (slab)	VH	k_V (cm/sec · 10^{-5} a 20°C)	H_2O	102900 ÷ 107000
	Enrobés Drainants	22,1	5,96		cores (slab)	VH	k_H (cm/sec · 10^{-5} a 5°C)	H_2O	72900 ÷ 73500
	Enrobés Drainants	22,1	5,96		cores (slab)	VH	k_H(cm/sec · 10^{-5} a 10°C)	H_2O	84700 ÷ 85900
	Enrobés Drainants	22,1	5,96		cores (slab)	VH	k_H (cm/sec · 10^{-5} a15°C)	H_2O	97050 ÷ 101200
	Enrobés Drainants	22,1	5,96		cores (slab)	VH	k_H (cm/sec · 10^{-5} a20°C)	H_2O	109400 ÷ 111200
	Enrobés Drainants	22,1	4,25		cores (slab)	VH	k_{Vintr} (cm^2·10^{-5}tra 5-20°C)	H_2O	1,076 ÷ 1,125
	Enrobés Drainants	22,1	5,96		cores (slab)	VH	k_{Hintr}(cm^2·10^{-5}tra 5-20°C)	H_2O	1,125 ÷ 1,142
(DI BENEDETTO et al., 1996a)	Enrobés Drainants	22,1	4,25		cores (slab)	VH	k_V (cm/sec · 10^{-5} a 0°C)	NaCl 23,3%	41600
	Enrobés Drainants	20,2 ÷ 22,1	4,09 ÷ 4,25		cores (slab)	VH	k_V (cm/sec · 10^{-5} a -5°C)	NaCl 23,3%	30600 ÷ 35000
	Enrobés Drainants	20,2 ÷ 22,1	4,09 ÷ 4,25		cores (slab)	VH	k_V (cm/sec ·10^{-5} a -10°C)	NaCl 23,3%	25450 ÷ 30600
	Enrobés Drainants	20,2 ÷ 22,1	4,09 ÷ 4,25		cores (slab)	VH	k_V (cm/sec ·10^{-5} a -15°C)	NaCl 23,3%	21800 ÷ 25700
	Enrobés Drainants	20,5 ÷ 22,1	5,94 ÷ 5,96		cores (slab)	VH	k_H (cm/sec ·10^{-5} a -5°C)	NaCl 23,3%	36050 ÷ 38400
	Enrobés Drainants	20,5 ÷ 22,1	5,94 ÷ 5,96		cores (slab)	VH	k_H (cm/sec·10^{-5} a -15°C)	NaCl 23,3%	27100 ÷ 28680
	Enrobés Drainants	22,1	4,25		cores (slab)	VH	k_V (cm/sec · 10^{-5} a 0°C)	NaCl 15%	50000
	Enrobés Drainants	22,1	4,25		cores (slab)	VH	k_V (cm/sec · 10^{-5} a -5°C)	NaCl 15%	41300
	Enrobés Drainants	22,1	4,25		cores (slab)	VH	k_V (cm/sec ·10^{-5} a -10°C)	NaCl 15%	37000
	Enrobés Drainants	22,1	4,25		cores (slab)	VH	k_V (cm/sec · 10^{-5} a 0°C)	$CaCl_2$ 32%	32700
	Enrobés Drainants	20,2 ÷ 22,1	4,09 ÷ 4,25		cores (slab)	VH	k_V (cm/sec · 10^{-5} a -5°C)	$CaCl_2$ 32%	25450 ÷ 28400
	Enrobés Drainants	20,2 ÷ 22,1	4,09 ÷ 4,25		cores (slab)	VH	k_V (cm/sec ·10^{-5} a -10°C)	$CaCl_2$ 32%	21100 ÷ 23400
	Enrobés Drainants	20,2 ÷ 22,1	4,09 ÷ 4,25		cores (slab)	VH	k_V (cm/sec ·10^{-5} a -15°C)	$CaCl_2$ 32%	18400 ÷ 20000
	Enrobés Drainants	20,5 ÷ 22,1	5,94 ÷ 5,96		cores (slab)	VH	k_H (cm/sec · 10^{-5} a -5°C)	$CaCl_2$ 32%	25000 ÷ 26300
	Enrobés Drainants	20,5 ÷ 22,1	5,94 ÷ 5,96		cores (slab)	VH	k_H (cm/sec·10^{-5} a -15°C)	$CaCl_2$ 32%	17600 ÷ 20000
	Enrobés Drainants	22,1	4,25		cores (slab)	VH	k_V (cm/sec · 10^{-5} a 0°C)	$MgCl_2$ 30%	15900
	Enrobés Drainants	20,2 ÷ 22,1	4,09 ÷ 4,25		cores (slab)	VH	k_V (cm/sec · 10^{-5} a -5°C)	$MgCl_2$ 30%	12000 ÷ 13600
	Enrobés Drainants	20,2 ÷ 22,1	4,09 ÷ 4,25		cores (slab)	VH	k_V (cm/sec ·10^{-5} a -10°C)	$MgCl_2$ 30%	10000 ÷ 10400
	Enrobés Drainants	20,2 ÷ 22,1	4,09 ÷ 4,25		cores (slab)	VH	k_V (cm/sec ·10^{-5} a -15°C)	$MgCl_2$ 30%	7700 ÷ 8400
	Enrobés Drainants	20,5 ÷ 22,1	5,94 ÷ 5,96		cores (slab)	VH	k_H (cm/sec · 10^{-5} a -5°C)	$MgCl_2$ 30%	11800 ÷ 15000
	Enrobés Drainants	20,5 ÷ 22,1	5,94 ÷ 5,96		cores (slab)	VH	k_H (cm/sec·10^{-5} a -15°C)	$MgCl_2$ 30%	7300 ÷ 9200
	Enrobés Drainants	20,5	5,94		cores (slab)	VH	k_H (cm/sec ·10^{-5} a -5°C)	$MgCl_2$ 31,7%	8500
	Enrobés Drainants	20,5	5,94		cores (slab)	VH	k_H (cm/sec·10^{-5} a -15°C)	$MgCl_2$ 31,7%	5000
	Enrobés Drainants	22,1	4,25		cores (slab)	VH	$k_{Vintr.}$(cm^2 ·10^{-5})	H_2O	1,1
	Enrobés Drainants	22,1	4,25		cores (slab)	VH	$k_{Vintr.}$(cm^2 ·10^{-5})	NaCl 15%	1,4
	Enrobés Drainants	22,1	4,25		cores (slab)	VH	$k_{Vintr.}$(cm^2 ·10^{-5})	NaCl 23,3%	1,4
	Enrobés Drainants	22,1	4,25		cores (slab)	VH	$k_{Vintr.}$(cm^2 ·10^{-5})	$CaCl_2$ 32%	2
	Enrobés Drainants	22,1	4,25		cores (slab)	VH	$k_{Vintr.}$(cm^2 ·10^{-5})	$MgCl_2$ 30%	3
(DI BENEDETTO et al., 1996b)	Enrobés Drainants	15,0 ÷ 22	4,00			PdC	k (cm/sec · 10^{-5})	H_2O	126000 ÷ 148000
	Enrobés Drainants	15,0 ÷ 22	4,00 ÷ 4,50			PdC	k (cm/sec · 10^{-5})	H_2O	11200 ÷ 14600
	Enrobés Drainants	19,6			core	VH	k_V (cm/sec · 10^{-5})	H_2O	11500
(CAVALIERE, 1997)	DRENANTE		3,00			PA	D^A (l/min)	H_2O	18
	DRENANTE	19,0				CHP (lab)	k (cm/sec · 10^{-5})	H_2O	75000
(MASCHIETT0, 1995)	DRENANTE						k (cm/sec · 10^{-5})	H_2O	130000
(CAFISO et al., 2000)	Congl. Bit. Chiuso					FHP	D (s)	H_2O	20 ÷ 140

(CAROTI et al.,1999)	DRENANTE	23,6 ÷ 27	5,00		Marshall sp.	CHP	K_{H} (cm/sec · 10^{-5})	H_2O	72570 ÷ 172500
	DRENANTE	23,6 ÷ 27	5,00		Marshall sp.	CHP	k_{V} (cm/sec · 10^{-5})	H_2O	45610 ÷ 129700
(GEORGIA)	OGFC					FHP	k (cm/sec · 10^{-5})	H_2O	4500
	OGFC (Modified)					FHP	k (cm/sec · 10^{-5})	H_2O	8450
	Porous Europ. Mix					FHP	k (cm/sec · 10^{-5})	H_2O	11574
(BRENGARTH et al., 1983)	Bétons Bit. 0-10					Drainoroute	CD (%)	H_2O	36 ÷ 85
	Bétons Bit. 0-14					Drainoroute	CD (%)	H_2O	51 ÷ 80
	Bét. Bit. Cloutés					Drainoroute	CD (%)	H_2O	60 ÷ 81
	Béton Ciment					Drainoroute	CD (%)	H_2O	57 ÷ 87
	Sables Enrobés					Drainoroute	CD (%)	H_2O	25 ÷ 53
	Bét. B. Recyclés					Drainoroute	CD (%)	H_2O	37 ÷ 48
	Bét. B. Drainants					Drainoroute	CD (%)	H_2O	64 ÷ 78
	Enr. Fins Cloutés					Drainoroute	CD (%)	H_2O	74 ÷ 81
	Coulis Bitumineux					Drainoroute	CD (%)	H_2O	65 ÷ 80

Tab 2: Review of HMA permeability and outflow times literature - continued

PAPER	PAVEMENT TYPE	AIR VOIDS (%)	THICKNESS RANGE (cm)	NMAS (mm)	COMPACTION PROCEDURE	DEVICE	INDICATOR	FLUID	INDICATOR RANGE
(PARIAT et al., 1992)	Enrobés Drainants	19,8 (Avg.)	4,00			Aut. P.	v_{q} (l/s·m^2)	H_2O	10 ÷ 25
(JIMENEZ et al., 1990)	Porous Asph. Mix.	4,0 ÷ 24,0		10		LCS P.	k (cm/sec · 10^{-5})	H_2O	200 ÷ 19000
	Porous Asph. Mix.	2,0 ÷ 20,0		12,5		LCS P.	k (cm/sec · 10^{-5})	H_2O	100 ÷ 16000
	Porous Asph. Mix.	2,0 ÷ 21,0		20		LCS P.	k (cm/sec · 10^{-5})	H_2O	200 ÷ 17000
(OLIVEIRA, 2003)	DRENANTE	22,8 ÷ 28,4				FHP	k_{V} (cm/sec · 10^{-5})	H_2O	38600 ÷ 45300
	DRENANTE	22,8 ÷ 28,4				FHP	k_{H} (cm/sec · 10^{-5})	H_2O	59700 ÷ 62800
(BELLANGER et al., 1999)	Enrobés Drainants					PdC	v_{p} (cm/sec)	H_2O	0,1 ÷ 1
(BROSSEAUD et al., 1997)	Enrobés Drainants	15 ÷ 22,5	2 ÷ 6			PdC	v_{p} (cm/sec)	H_2O	0,6 ÷ 1,6

SYMBOLS
AIP = Air-induced Permeameter; ARZ = Above Restricted Zone; Aut. P. = Automatic Permeameter; BRZ = Below Restricted Zone; CD = “Drainoroute” coefficient; CHP = Constant Head Permeameter; Coarse-Graded M = Coarse-Graded Mix with Modified Asphalt; D = drainability; D^{A} = “Autostrade” drainability; FHP = Falling-Head Permeameter; FHT = Falling-Head Test; FWP(D5084) = Flexible Wall Permeameter (ASTM D 5084); FWP (FM 5-565) = Flexible Wall Permeameter (FM 5-565); the standard (FM 5-565) is similar to (Virginia Test Methods-120); FWP (PS 129) = Flexible Wall Permeameter (ASTM PS 129); k = permeability; $k_{crit.}$ = critical permeability; k_{H} = horizontal permeability; $k_{Hintr.}$ = horizontal intrinsic permeability; k_{V} = vertical permeability; $k_{Vintr.}$ = vertical intrinsic permeability; NCAT = National Center Asphalt Transportation Permeameter; LCS P. = Laboratorio de Caminos de Santander Permeameter; NMAS = Nominal Maximum Aggregate Size; PA = “Autostrade” Permeameter; PdC = Falling Head Permeameter (“de chantier”); SGC = Superpave Giratory Compactor; SR = Steel Roller; SRT = Steel/Rubber Tire Roller; SVC = Superpave Vibratory Compactor; SWR = Steel Wheel Roller; V = Vacuum reading; VH = VH Permeameter; v_{p} = average percolation velocity; v_{q} = velocity (connected with rate flow); WPIP = Worcester Polytechnic Institute Permeameter;

Tab 3: Review of air voids/permeability influence on mechanical properties

PAPER	PAVEMENT TYPE	AIR VOIDS/ PERMEABILITY	MECHANICAL PARAMETER/ PROPERTY
(HUNTER et al., 2001)	Hot Mix Asphalt mixtures	Air voids	Rutting, Indirect Tensile Strength (after freeze-thaw cycles)
(WOLTERS, 2003)	Hot Mix Asphalt mixtures	Air voids	Raveling
(NCHRP, 2002b)	Hot Mix Asphalt mixtures	Air voids	Fatigue-Cracking, Rutting, Modulus
(NCHRP, 2002a)	Hot Mix Asphalt mixtures	Air voids	Indirect Tensile Strength, Moduli, Rutting, Fatigue Life
(CASTELBLANCO et al., 2005)	Hot Mix Asphalt mixtures	Air voids	Moisture Damage (evaluated using ER (“Energy Ratio”) and N_{f} (number of cycles to grow a one-inch long crack under cyclic loading in the Superpave IDT – Indirect Tension Test))
(KANDHAL, 1990)	Hot Mix Asphalt mixtures	Air voids	Rutting
(KANDHAL et al., 1996)	Hot Mix Asphalt mixtures	Air voids	Resilient Modulus, Tensile Strength (after aging)
(KANDHAL et al., 1998)	Hot Mix Asphalt mixtures	Air voids	Rutting, Shoving
(MAHER et al., 2001)	Hot Mix Asphalt mixtures	Air voids	Rutting, Fatigue Cracking
(KANDHAL et al., 1993)	Hot Mix Asphalt mixtures	Air voids	Rutting
(KANDHAL et al., 1995)	Recycled HMA	Air voids	Rutting, Raveling, Fatigue Cracking, Indirect Tensile Strength
(AUSTROADS, 1999)	Dense Graded Asphalt Mix	Air voids	Rutting, Fatigue Life, Strength/Stiffness, Bitumen Viscosity, Raveling
(PROWELL, 2000)	Hot Mix Asphalt mixtures	Air voids	Rutting
(HARVEY et al., 1995)	Asphalt Concrete mix	Air voids	Fatigue Life, Stiffness
(KENNEDY et al., 1990)		Air voids	Strength, Modulus
(PELLAND et al., 2003)	Stone Mastic Asphalt (SMA), Reclaimed asphalt pav. (RAP), Rosphalt 50^{TM}	Air voids	Rutting, Resilient Modulus

(JIMENEZ et al., 1990)	Porous Asphalt Mixes	Air voids	Abrasion Loss
(MALLICK et al., 2000) (KANDHAL et al., 1999) (COOLEY et al., 2000)	OGFC	Air voids/ Permeability	Abrasion Loss, Aging, Moisture Damage (Indirect Tensile Strength after freeze/thaw cycles), Rutting, Cracking, Raveling, Surface Texture
(FAGHRI et al., 2002)	OGFC	Permeability	Indirect Tensile Strength
(POULIKAKOS et al., 2004)	Porous Asphalt	Air voids/ Permeability	Indirect Tensile Strength, Rutting, Abrasion Loss